Supporting Information

Strained Azabora[2]ferrocenophanes

Hridaynath Bhattacharjee,[†] Subhayan Dey,[†,°] Jianfeng Zhu,[ϕ] Wei Sun,[ϕ,§] and Jens Müller*,[†]

[†] Department of Chemistry and [ϕ] Saskatchewan Structural Sciences Centre, University of Saskatchewan, 110 Science Place, Saskatoon, Saskatchewan S7N 5C9, Canada.

[°] Department of Inorganic Chemistry, Karlsruhe Institute of Technology (KIT), Geb. 30.45, Engesserstr. 15, 76131, Karlsruhe, Germany.

[§] Research and Development Center, Fuyao Group Gongye Cun, Shanghang North Road, Fuqing 350301, Fuzhou, Fujian Province, People's Republic of China.

Table of Contents

Experimental Section

General Methods. If not mentioned otherwise, all syntheses were carried out using standard Schlenk and glovebox techniques. Solvents were dried using an MBraun Solvent Purification System and stored under nitrogen over 3 Å molecular sieves. C_6D_6 for NMR spectroscopy was degassed by freeze-pump-thaw cycles and stored under nitrogen over 3 Å molecular sieves. Unless otherwise noted, temperatures refer to that of the bath (e.g., dry ice/acetone bath for –78 °C).

Characterization Methods. ^{1}H, ^{11}B, and ^{13}C NMR spectra were recorded on 500 MHz Bruker Avance, 500 MHz Bruker Avance III HD, and 600 MHz Bruker Avance III HD NMR spectrometers at 25 ºC in C_6D_6. ^{1}H chemical shifts are referenced to the residual protons of the deuterated solvent C_6D_6 at δ = 7.15 ppm; ^{13}C chemical shifts are referenced to the C_6D_6 signal at δ = 128.00 ppm. ^{11}B NMR spectra were calibrated using $F_3B{\cdot}OEt_2$ (0.0 ppm) as external reference. The following abbreviations are used to described NMR signals: s (singlet), d (doublet), pst (pseudo triplet), sept (septet), br (broad). Some Cp protons appear as slightly broadened singlets, while others appear as pseudo triplets. Coupling constants obtained from ^{1}H NMR spectra are associated with an error and reported to the first decimal point (the digital resolution in ^{1}H NMR spectra is 0.2 Hz). Assignments for newly synthesized compounds were supported by additional NMR experiments (COSY, HMQC, HMBC, and DEPT). High resolution mass data were obtained with a JEOL AccuTOF GCv 4G instrument using field desorption ionization (FDI). For the isotopic pattern, only the mass peak of the isotopoloque or isotope with the highest natural abundance is listed. Elemental analyses were performed on a Perkin Elmer 2400 CHN Elemental Analyzer. Differential Scanning Calorimetry (DSC) analyses were performed on a TA Instrument Q20 at a heating rate of 10 °C min^{-1}. Samples, sealed in hermetic aluminum pans, were tared using a balance with a repeatability of 0.1 mg (AB204-S Mettle Toledo). For each run, around 3 mg of a sample was measured. The known melting enthalpy of a sample of indium was used to check on the calibration of the DSC instrument. DSC data was analyzed with TA Instruments Universal Analysis 2000 software. After each DSC run, the content of the pan was dissolved in organic solvent under inert atmosphere and a ^{1}H NMR spectrum of the solution showed mainly unaltered starting material, which revealed that thermal ROP did not occur.

Reagents. Dichloro(diisopropylamino)borane,[1] dichloro[tris(trimethylsily)methyl]borane,[2] 1-bromo-1'-(trimethylsilylamino)ferrocene (**1a**),[3] and 1-bromo-1'-(neopentylamino)ferrocene (**1b**)[4] were synthesized as reported. For **1a** and **1b** please note that small amounts the impurity $CpFeC_5H_4NHR$ are present (see references 3 and 4 for details). However, molar amounts were calculated as if these starting materials were absolutely pure. The reagent *n*BuLi (2.5 M in hexanes) was purchased from Sigma Aldrich.

Synthesis of azabora[2]ferrocenophane 2a.

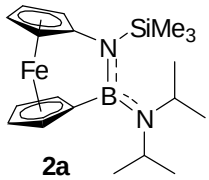

2a

*n*BuLi (2.5 M in hexanes, 0.41 mL, 1.0 mmol) was added dropwise to a –78 ºC cooled solution of 1-bromo-1'-(trimethylsilylamino)ferrocene **1a** (0.171 g, 0.486 mmol) in a solvent mixture of hexanes and thf (10 mL; hexanes/thf; 9/1), resulting in a color change from pale yellow to bright orange. After the reaction mixture was stirred for 40 min at –78 °C, the dry ice bath was replaced by an ice bath, followed by stirring of the reaction mixture at 0 °C for 1 h. A solution of iPr$_2$NBCl$_2$ (0.090 g, 0.49 mmol) in hexanes (6.0 mL) was added dropwise over 2 min. The reaction mixture was warmed to ambient temperature and stirred for 1 h. After all volatiles were removed under high vacuum, the product was dissolved in hexanes (15 mL) and LiCl was removed by Schlenk filtration and the white residue was washed with more hexanes (2 × 2.0 mL). From this red filtrate, residual solvents were removed under high vacuum, resulting in a red sticky solid. Product **2a** was obtained by vacuum sublimation (60 °C; p ~ 10^{-2} mbar) in form of red crystals (0.103 g, 55%). ^{1}H NMR (C$_6$D$_6$, 500.1 MHz): δ 0.26 (s, 9H, Si(CH$_3$)$_3$), 1.20 (d, J_{HH} = 6.8 Hz, 12H, N[CH(C$\underline{H}_3$)$_2$]$_2$), 3.72 (sept, J_{HH} = 6.7 Hz, 2H, N[C$\underline{H}$(CH$_3$)$_2$]$_2$), 3.91 (pst, 2H, α-H of Cp^N), 4.21 (pst, 2H, α-H of Cp^B), 4.27 (pst, 2H, β-H of Cp^N), 4.53 (pst, 2H, β-H of Cp^B). ^{13}C{^{1}H} NMR (C$_6$D$_6$, 125.8 MHz): δ 2.4 (Si(CH$_3$)$_3$), 25.0 (N[CH($\underline{C}$H$_3$)$_2$]$_2$), 47.8 (N[$\underline{C}$H(CH$_3$)$_2$]$_2$), 67.6 (α-C of Cp^N), 70.6 (α-C of Cp^B), 72.8 (β-C of Cp^N), 76.3 (β-C of Cp^B), 86.4 (*ipso*-C of Cp^B), 98.4 (*ipso*-C of Cp^N). ^{11}B NMR (C$_6$D$_6$, 160.5 MHz): δ 34.2 ppm. HRMS (FDI): *m*/*z* calcd for C$_{19}$H$_{31}$BFeN$_2$Si, 382.1699; found 382.1707. Elemental anal. calcd (%) for C$_{19}$H$_{31}$BFeN$_2$Si (382.211): C, 59.71; H, 8.18; N, 7.33. Found: C, 59.61; H, 8.33; N, 7.23.

Synthesis of azabora[2]ferrocenophane 2b.

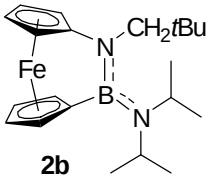

2b

*n*BuLi (2.4 M in hexanes, 0.72 mL, 1.7 mmol) was added dropwise to a –78 ºC cooled solution of 1-bromo-1'-(neopentylamino)ferrocene (**1b**) (0.287 g, 0.820 mmol) in a solvent mixture of hexanes and thf (15 mL; hexanes/thf; 9/1), resulting in a color change from pale yellow to bright orange. After the reaction mixture was stirred for 40 min at –78 ºC, the dry ice bath was replaced by an ice bath, followed by stirring of the reaction mixture at 0 °C for 1 h. A solution of iPr$_2$NBCl$_2$ (0.165 g, 0.907 mmol) in hexanes (7.5 mL) was added dropwise over 2 min. The reaction mixture was warmed to ambient temperature and stirred for 1 h. After all volatiles were removed under high vacuum, the product was dissolved in hexanes (20 mL) and LiCl was removed by a Schlenk filtration and the white residue was washed with more hexanes (2 × 2.0 mL). From this red filtrate, residual solvents were removed under high vacuum, resulting in a red sticky solid. Product **2b** was obtained by crystallization in hexanes at –80 °C in form of red crystals (0.217 g, 70%). ^{1}H NMR (C$_6$D$_6$, 500.3 MHz): δ 0.97 (s, 9H, C(CH$_3$)$_3$), 1.20 (d, J_{HH} = 6.6 Hz, 12H, N[CH(C$\underline{H}_3$)$_2$]$_2$), 3.10 [s, 2H, NCH$_2$], 3.53 (sept, J_{HH} = 6.7 Hz, 2H, N[C$\underline{H}$(CH$_3$)$_2$]$_2$), 3.90 (pst, 2H, α-H of Cp^N), 4.20 (pst, 2H, α-H of Cp^B), 4.42 (pst, 2H, β-H of Cp^N), 4.54 (pst, 2H, β-H of Cp^B).

$^{13}C\{^1H\}$ NMR (C_6D_6, 125.8 MHz): δ 24.4 ($C(\underline{C}H_3)_3$), 29.4 ($N[CH(\underline{C}H_3)_2]_2$), 32.9 ($CH_2\underline{C}(CH_3)_3$), 46.2 ($N[\underline{C}H(CH_3)_2]_2$), 62.5 ($NCH_2$), 67.4 ($\alpha$-C of Cp^N), 70.4 (α-C of Cp^B), 71.4 (β-C of Cp^N), 76.1 (β-C of Cp^B), 83.0 (*ipso*-C of Cp^B), 104.0 (*ipso*-C of Cp^N). ^{11}B NMR (C_6D_6, 160.5 MHz): δ 33.3 ppm. HRMS (FDI): *m/z* calcd for $C_{21}H_{33}BFeN_2$, 380.2086; found 380.2072. Elemental anal. calcd (%) for $C_{21}H_{33}BFeN_2$ (380.164): C, 66.35; H, 8.75; N, 7.37; found: C, 66.52; H, 8.96; N, 6.94.

Synthesis of azabora[2]ferrocenophane 2c.

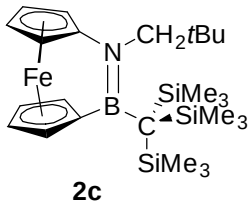

2c

*n*BuLi (2.4 M in hexanes, 0.41 mL, 0.98 mmol) was added dropwise to a –78 ºC cooled solution of 1-bromo-1'-(neopentylamino)ferrocene (**1b**) (0.161 g, 0.460 mmol) in a solvent mixture of hexanes and thf (10 mL; hexanes/thf; 9/1), resulting in a color change from pale yellow to bright orange. After the reaction mixture was stirred for 40 min at –78 ºC, the dry ice bath was replaced by an ice bath, followed by stirring of the reaction mixture at 0 °C for 1 h. A solution of $[(Me_3Si)_3C]BCl_2$ (0.156 g, 0.498 mmol) in hexanes (5.0 mL) was added dropwise over 2 min. The reaction mixture was warmed to ambient temperature and stirred for 1 h. After all volatiles were removed under high vacuum, the product was dissolved in hexanes (15 mL), LiCl was removed by a Schlenk filtration, and the white residue was washed with more hexanes (2 × 2.0 mL). From this red filtrate, residual solvents were removed under high vacuum, resulting in a red oil. Product **2c** was obtained by crystallization in hexanes at –80 °C in form of red crystals (0.160 g, 68%). ^1H NMR (C_6D_6, 600.2 MHz): δ 0.39 (s, 27H, $C[Si(CH_3)_3]_3$), 0.94 (s, 9H, $C(CH_3)_3$), 3.41 (s, 2H, NCH_2), 3.81 (s, br, 2H, α-H of Cp^N), 4.06 (s, br, 2H, α-H of Cp^B), 4.34 (s, br, 2H, β-H of Cp^N), 4.39 (s, br, 2H, β-H of Cp^B). $^{13}C\{^1H\}$ NMR (C_6D_6, 150.9 MHz): δ 7.9 ($C[Si(\underline{C}H_3)_3]_3$), 14.1 ($\underline{C}[Si(CH_3)_3]_3$), 29.7 ($C(\underline{C}H_3)_3$), 32.8 ($\underline{C}(CH_3)_3$), 63.7 ($NCH_2$), 67.4 ($\alpha$-C of Cp^N), 69.9 (α-C of Cp^B), 71.4 (β-C of Cp^N), 75.4 (β-C of Cp^B), 82.9 (*ipso*-C of Cp^B), 103.8 (*ipso*-C of Cp^N). ^{11}B NMR (C_6D_6, 192.6 MHz): δ 49.0 ppm. HRMS (FDI): *m/z* calcd for $C_{25}H_{46}BFeNSi_3$, 511.2381; found 511.2401. Elemental anal. calcd (%) for $C_{25}H_{46}BFeNSi_3$ (511.560): C, 58.70; H, 9.06; N, 2.74; found: C, 58.62; H, 9.36; N, 2.73.

Attempted Thermal ROP of 2b. Compound **2b** (0.023 g, 0.061 mmol) was taken in a vacuum-sealed NMR tube and heated at 200 °C and 250 °C for 1 h each and then at 300 °C for 4 h. ^1H NMR spectroscopy (see Figure S14) of the resulting solid showed mainly the presence of the unaltered starting material **2b**. New signals at δ 0.95, 2.77, and 4.23 ppm were present, possibly indicating the generation of new species caused by heat. The experiment was then repeated as following.

Compound **2b** (0.018 g, 0.047 mmol) was taken in a vacuum-sealed NMR tube and heated at 300 °C for an extended period of 22 h. A ^1H NMR spectrum of the reaction displayed similar signals to those previously observed (see Figure S15). The new signals did not show any increase in their relative intensities. This may indicate that the new unknown compound(s) is(are) probably forming due to the residual moisture left in the NMR tube and not due to any thermal reactivity.

Crystal Structure Determination of 2a–c. Single crystals were coated with Paratone-N oil, mounted using a micromount (MiTeGen - Microtechnologies for Structural Genomics), and frozen in the cold stream of an Oxford Cryojet attached to the diffractometer. Crystal data were collected on a Bruker APEX II diffractometer at –100 °C using monochromated Mo Kα radiation (λ = 0.71073 Å). An initial orientation matrix and cell was determined by ω scans, and the X-ray data were measured using ϕ and ω scans.[5] Frames were integrated with the Bruker SAINT software package[6] and data reduction was performed with the *APEX2* software package.[5] A multi-scan absorption correction (SADABS) was applied.[6] The structures were solved by the Intrinsic Phasing method implemented with SHELXT and refined using the Bruker SHELXTL software package.[7] Non-hydrogen atoms were refined with independent anisotropic displacement parameters. Hydrogen atoms were placed at geometrically idealized positions (riding model) and their displacement parameters were fixed to be 20 or 50% larger than those of the attached non-hydrogen atoms. Crystallographic data are summarized in Table S1, while bond lengths and bond angles are shown in Table S2–S4. Crystallographic data were submitted to the Cambridge Crystallographic Data Centre (**2a**–**c**: CCDC 1825153–1825155). The ellipsoid plots were prepared using ORTEP-3 for Windows.[8] The common set of distortion angles was calculated using the program PLATON.[9] The esds of all distortion angles that involve centroids of Cp rings (β, δ, τ) might be somewhat smaller than they should be, as esds on centroids were not included in the calculation.

DFT Calculations. All calculations were done employing the software package GAUSSIAN 09.[10] Geometries were optimized at the B3PW91/6-311+G(d,p) level.[11] The B3PW91 functional had been chosen based on the benchmark investigation of Grimme *et al.*,[12] as well as our recent application to [1]FCPs.[13] Frequency calculations were used to confirm minima. An ultrafine grid (int=ultrafine) and tight requirements for geometry optimizations (opt=tight) were used for all calculations. Structural parameters from the calculated coordinates were extracted with the help of Mercury (version 3.9)[14] and CYLview (version 1b)[15].

For products of type **4** (see eq 2) different isomers of very similar enthalpies were optimized and only the one resulting in the largest heat release were taken into consideration. The difference between isomers is due to different conformations of the amino and/or boryl groups with respect to the ferrocene moiety. However, differences for the different isomers in each series were very small (in kJ mol^{-1}; **4a**: -69.3 to -70.6; **4b**: -67.6 to -68.7; **4c**: -102.0 to -102.8; **4d**: -71.4 to -71.7; **4e** (CC case): -84.7 to -84.9). Please note that different isomers with respect to rotation about the Fe-$Cp^{centriod}$ bonds were not considered. For all isomers of type **4** the relative positions of amino to boryl groups were the same. See the attached file for calculated Cartesian coordinates of the considered isomers.

References

[1] W. Gerrard, H. R. Hudson and E. F. Mooney, *J. Chem. Soc.* **1960**, 5168.

[2] (a) S. S. Al-Juaid, C. Eaborn, M. N. A. El-Kheli, P. B. Hitchcock, P. D. Lickiss, M. E. Molla, J. D. Smith and J. A. Zora, *J. Chem. Soc., Dalton Trans.*, **1989**, 447; (b) A. Tapper, Dissertation, 1988, RWTH Aachen.

[3] S. Dey, J. W. Quail and J. Müller, *Organometallics* 2015, **34**, 3039.

[4] S. Dey, W. Sun and J. Müller, *Inorg. Chem.* 2016, **55**, 3630.

[5] Bruker, 2014.3-0 ed., Bruker AXS Inc., Madison, Wisconsin, **2014**.

[6] Bruker, v8.34a ed., Bruker AXS Inc., Madison, WI, USA, **2013**.

[7] (a) G. M. Sheldrick, University of Göttingen, Germany; (b) G. M. Sheldrick, *Acta Crystallogr., Sec A* 2008, **64**, 112.

[8] L. J. Farrugia, *J. Appl. Crystallogr.* 1997, **30**, 565.

[9] A. L. Spek, University of Utrecht, The Netherlands, **2011**.

[10] M. J. Frisch, G. W. Trucks, H. B. Schlegel, G. E. Scuseria, M. A. Robb, J. R. Cheeseman, G. Scalmani, V. Barone, B. Mennucci, G. A. Petersson, H. Nakatsuji, M. Caricato, X. Li, H. P. Hratchian, A. F. Izmaylov, J. Bloino, G. Zheng, J. L. Sonnenberg, M. Hada, M. Ehara, K. Toyota, R. Fukuda, J. Hasegawa, M. Ishida, T. Nakajima, Y. Honda, O. Kitao, H. Nakai, T. Vreven, J. J. A. Montgomery, J. E. Peralta, F. Ogliaro, M. Bearpark, J. J. Heyd, E. Brothers, K. N. Kudin, V. N. Staroverov, T. Keith, R. Kobayashi, J. Normand, K. Raghavachari, A. Rendell, J. C. Burant, S. S. Iyengar, J. Tomasi, M. Cossi, N. Rega, J. M. Millam, M. Klene, J. E. Knox, J. B. Cross, V. Bakken, C. Adamo, J. Jaramillo, R. Gomperts, R. E. Stratmann, O. Yazyev, A. J. Austin, R. Cammi, C. Pomelli, J. W. Ochterski, R. L. Martin, K. Morokuma, V. G. Zakrzewski, G. A. Voth, P. Salvador, J. J. Dannenberg, S. Dapprich, A. D. Daniels, O. Farkas, J. B. Foresman, J. V. Ortiz, J. Cioslowski and D. J. Fox, Revision E.01 ed., Gaussian, Inc., Wallingford CT, **2013**.

[11] (a) J. P. Perdew, in *Electronic Structure of Solids '91* (Eds.: P. Ziesche, H. Eschrig), Akademie Verlag, Berlin, **1991**, pp. 11-20; (b) J. P. Perdew, J. A. Chevary, S. H. Vosko, K. A. Jackson, M. R. Pederson, D. J. Singh and C. Fiolhais, *Phys. Rev. B* 1992, **46**, 6671; (c) J. P. Perdew, J. A. Chevary, S. H. Vosko, K. A. Jackson, M. R. Pederson, D. J. Singh and C. Fiolhais, *Phys. Rev. B* 1993, **48**, 4978; (d) A. D. Becke, *J. Chem. Phys.* 1993, **98**, 5648; (e) J. P. Perdew, K. Burke and Y. Wang, *Phys. Rev. B* 1996, **54**, 16533; (f) K. Burke, J. P. Perdew and Y. Wang, in *Electronic Density Functional Theory: Recent Progress and New Directions* (Eds.: J. F. Dobson, G. Vignale, M. P. Das), Plenum, **1998**, pp. 81-111.

[12] L. Goerigk and S. Grimme, *Phys. Chem. Chem. Phys.* 2011, **13**, 6670.

[13] (a) H. Bhattacharjee and J. Müller, *Coord. Chem. Rev.* 2016, **314**, 114; b) E. Khozeimeh Sarbisheh, J. Esteban Flores, J. Zhu and J. Müller, *Chem. Eur. J.* 2016, **22**, 16838; c) E. Khozeimeh Sarbisheh, H. Bhattacharjee, M. P. T. Cao, J. Zhu and J. Müller, *Organometallics* 2017, **36**, 614; d) E. Khozeimeh Sarbisheh, J. Esteban Flores, B. J. Anderson, J. Zhu and J. Müller, *Organometallics* 2017, **36**, 2182.

[14] Mercury, http://www.ccdc.cam.ac.uk/mercury.

[15] C. Y. Legault, *1.0b*, Université de Sherbrooke, **2009**.

Table S1. Crystal and Structural Refinement Data for Compound **2a–c**.

Compound name	**2a**	**2b**	**2c**
CCDC	1825153	1825154	1825155
empirical formula	$C_{19}H_{31}BFeN_2Si$	$C_{21}H_{33}BFeN_2$	$C_{25}H_{46}BFeNSi_3$
Fw / g mol^{-1}	382.21	380.16	511.56
cryst. size / mm^3	0.450 × 0.300 × 0.150	0.390 × 0.260 × 0.250	0.420 x 0.250 x 0.140
cryst. system	monoclinic	monoclinic	monoclinic
space group	$P2_1/n$	$P2_1/n$	$P2_1/c$
Z	4	4	4
a / Å	6.3615(4)	6.2078(2)	16.4880(7)
b / Å	19.7152(13)	20.6010(7)	9.3747(4)
c / Å	15.9518(11)	15.7389(6)	18.1053(7)
α / °	90	90	90
β / °	94.707(2)	94.438(2)	95.939(2)
γ / °	90	90	90
volume / Å^3	1993.9(2)	2006.76(12)	2783.5(2)
ρ_{calc} / g cm^{-3}	1.273	1.258	1.221
temperature / K	173(2)	173(2)	173(2)
μ_{calc}./ mm^{-1}	0.819	0.757	0.684
θ range / °	3.292 to 28.896	2.596 to 30.080	2.449 to 29.136
completeness / %	99.8	99.9	99.9
collected reflections	27888	44868	28647
independent reflections	5192 [R(int) = 0.0484]	5890 [R(int) = 0.0318]	7484 [R(int) = 0.0415]
absorption correction	multi-scan	multi-scan	multi-scan
data / restraints / params	5192 / 0 / 224	5890 / 0 / 272	7484 / 0 / 292
goodness-of-fit	1.064	1.034	1.046
R_1 [I > 2 σ(I)][a]	0.0375	0.0368	0.0376
wR_2 (all data)[a]	0.1057	0.0883	0.0951
largest diff. peak and hole, $\Delta\rho_{elect}$ / e Å^{-3}	0.966 and –0.329	0.597 and –0.363	0.435 and –0.312

[a] $R_1 = [\Sigma||F_o|-|F_c||]/[\Sigma|F_o|]$ for $[F_o^2 > 2\sigma(F_o^2)]$, $wR_2 = \{[\Sigma w(F_o^2-F_c^2)^2]/[\Sigma w(F_o^2)^2]\}^{1/2}$ [all data].

Table S2. Bond Lengths (Å) and Bond Angles (deg) for Compound **2a**.

Fe(1)-C(1)	1.9625(17)	C(6)-Fe(1)-C(5)	107.96(8)	C(5)-C(1)-C(2)	107.24(16)
Fe(1)-C(6)	1.9770(18)	C(10)-Fe(1)-C(5)	145.37(8)	C(5)-C(1)-N(1)	126.37(17)
Fe(1)-C(10)	2.0138(19)	C(7)-Fe(1)-C(5)	100.87(8)	C(2)-C(1)-N(1)	126.00(16)
Fe(1)-C(7)	2.0151(19)	C(2)-Fe(1)-C(5)	69.60(9)	C(5)-C(1)-Fe(1)	71.19(10)
Fe(1)-C(2)	2.0197(19)	C(1)-Fe(1)-C(3)	70.39(8)	C(2)-C(1)-Fe(1)	71.06(10)
Fe(1)-C(5)	2.0223(19)	C(6)-Fe(1)-C(3)	147.75(8)	N(1)-C(1)-Fe(1)	117.54(12)
Fe(1)-C(3)	2.060(2)	C(10)-Fe(1)-C(3)	124.08(10)	C(1)-C(2)-C(3)	107.96(18)
Fe(1)-C(9)	2.062(2)	C(7)-Fe(1)-C(3)	166.26(9)	C(1)-C(2)-Fe(1)	66.79(10)
Fe(1)-C(4)	2.067(2)	C(2)-Fe(1)-C(3)	41.17(8)	C(3)-C(2)-Fe(1)	70.92(11)
Fe(1)-C(8)	2.0670(19)	C(5)-Fe(1)-C(3)	68.62(9)	C(4)-C(3)-C(2)	108.20(18)
Si(1)-N(1)	1.7823(16)	C(1)-Fe(1)-C(9)	148.27(8)	C(4)-C(3)-Fe(1)	70.17(11)
Si(1)-C(13)	1.862(2)	C(6)-Fe(1)-C(9)	70.97(8)	C(2)-C(3)-Fe(1)	67.91(11)
Si(1)-C(11)	1.864(2)	C(10)-Fe(1)-C(9)	40.98(8)	C(3)-C(4)-C(5)	108.00(18)
Si(1)-C(12)	1.866(2)	C(7)-Fe(1)-C(9)	68.87(9)	C(3)-C(4)-Fe(1)	69.65(12)
N(1)-C(1)	1.455(2)	C(2)-Fe(1)-C(9)	123.94(9)	C(5)-C(4)-Fe(1)	67.91(11)
N(1)-B(1)	1.472(2)	C(5)-Fe(1)-C(9)	166.41(9)	C(4)-C(5)-C(1)	108.49(18)
N(2)-B(1)	1.419(2)	C(3)-Fe(1)-C(9)	119.84(9)	C(4)-C(5)-Fe(1)	71.25(11)
N(2)-C(17)	1.477(2)	C(1)-Fe(1)-C(4)	70.27(8)	C(1)-C(5)-Fe(1)	66.72(10)
N(2)-C(14)	1.482(2)	C(6)-Fe(1)-C(4)	148.73(8)	C(10)-C(6)-C(7)	105.36(16)
C(1)-C(5)	1.432(3)	C(10)-Fe(1)-C(4)	164.25(9)	C(10)-C(6)-B(1)	126.57(16)
C(1)-C(2)	1.433(3)	C(7)-Fe(1)-C(4)	126.11(9)	C(7)-C(6)-B(1)	125.56(17)
C(2)-C(3)	1.435(3)	C(2)-Fe(1)-C(4)	68.86(9)	C(10)-C(6)-Fe(1)	70.14(11)
C(3)-C(4)	1.418(3)	C(5)-Fe(1)-C(4)	40.84(8)	C(7)-C(6)-Fe(1)	70.16(11)
C(4)-C(5)	1.427(3)	C(3)-Fe(1)-C(4)	40.18(9)	B(1)-C(6)-Fe(1)	110.24(12)
C(6)-C(10)	1.445(3)	C(9)-Fe(1)-C(4)	138.30(8)	C(8)-C(7)-C(6)	109.36(18)
C(6)-C(7)	1.447(3)	C(1)-Fe(1)-C(8)	149.09(8)	C(8)-C(7)-Fe(1)	71.47(11)
C(6)-B(1)	1.613(3)	C(6)-Fe(1)-C(8)	70.90(8)	C(6)-C(7)-Fe(1)	67.35(10)
C(7)-C(8)	1.429(3)	C(10)-Fe(1)-C(8)	68.75(8)	C(9)-C(8)-C(7)	107.87(17)
C(8)-C(9)	1.424(3)	C(7)-Fe(1)-C(8)	40.96(8)	C(9)-C(8)-Fe(1)	69.66(11)
C(9)-C(10)	1.428(3)	C(2)-Fe(1)-C(8)	164.27(9)	C(7)-C(8)-Fe(1)	67.57(10)
C(14)-C(15)	1.522(3)	C(5)-Fe(1)-C(8)	126.11(8)	C(8)-C(9)-C(10)	107.84(18)
C(14)-C(16)	1.525(3)	C(3)-Fe(1)-C(8)	138.33(8)	C(8)-C(9)-Fe(1)	70.00(11)
C(17)-C(19)	1.531(3)	C(9)-Fe(1)-C(8)	40.34(9)	C(10)-C(9)-Fe(1)	67.68(11)
C(17)-C(18)	1.532(3)	C(4)-Fe(1)-C(8)	121.50(8)	C(9)-C(10)-C(6)	109.49(17)
		N(1)-Si(1)-C(13)	108.51(9)	C(9)-C(10)-Fe(1)	71.34(11)
C(1)-Fe(1)-C(6)	85.88(7)	N(1)-Si(1)-C(11)	112.28(10)	C(6)-C(10)-Fe(1)	67.42(10)
C(1)-Fe(1)-C(10)	107.48(8)	C(13)-Si(1)-C(11)	105.93(13)	N(2)-C(14)-C(15)	112.91(16)
C(6)-Fe(1)-C(10)	42.45(8)	N(1)-Si(1)-C(12)	112.80(9)	N(2)-C(14)-C(16)	114.87(16)
C(1)-Fe(1)-C(7)	108.22(8)	C(13)-Si(1)-C(12)	106.03(13)	C(15)-C(14)-C(16)	111.95(18)
C(6)-Fe(1)-C(7)	42.48(7)	C(11)-Si(1)-C(12)	110.84(11)	N(2)-C(17)-C(19)	112.03(19)
C(10)-Fe(1)-C(7)	69.62(8)	C(1)-N(1)-B(1)	112.58(14)	N(2)-C(17)-C(18)	112.88(18)
C(1)-Fe(1)-C(2)	42.16(8)	C(1)-N(1)-Si(1)	109.55(11)	C(19)-C(17)-C(18)	112.08(19)
C(6)-Fe(1)-C(2)	106.73(8)	B(1)-N(1)-Si(1)	137.86(13)	N(2)-B(1)-N(1)	126.27(17)
C(10)-Fe(1)-C(2)	98.71(9)	B(1)-N(2)-C(17)	123.30(16)	N(2)-B(1)-C(6)	119.98(16)
C(7)-Fe(1)-C(2)	145.08(8)	B(1)-N(2)-C(14)	123.62(16)	N(1)-B(1)-C(6)	113.74(15)
C(1)-Fe(1)-C(5)	42.09(7)	C(17)-N(2)-C(14)	113.05(15)		

Table S3. Bond Lengths (Å) and Bond Angles (deg) for Compound **2b**.

Fe(1)-C(1)	1.9517(14)	Fe(1)-C(8)	2.0662(15)	N(2)-C(16)	1.4891(19)
Fe(1)-C(6)	1.9880(13)	N(1)-C(1)	1.453(4)	B(1)-C(6)	1.603(2)
Fe(1)-C(10)	2.0111(15)	N(1)-B(1)	1.453(4)	C(1)-C(5)	1.426(2)
Fe(1)-C(2)	2.0118(15)	N(1)-C(11)	1.470(4)	C(1)-C(2)	1.428(2)
Fe(1)-C(5)	2.0157(16)	N(1')-C(1)	1.473(7)	C(2)-C(3)	1.421(2)
Fe(1)-C(7)	2.0210(14)	N(1')-C(11')	1.474(8)	C(3)-C(4)	1.411(3)
Fe(1)-C(3)	2.0604(15)	N(1')-B(1)	1.528(7)	C(4)-C(5)	1.422(2)
Fe(1)-C(9)	2.0640(15)	N(2)-B(1)	1.4137(19)	C(6)-C(7)	1.442(2)
Fe(1)-C(4)	2.0648(15)	N(2)-C(19)	1.4744(19)	C(6)-C(10)	1.445(2)

C(7)-C(8)	1.429(2)	C(10)-Fe(1)-C(4)	165.01(7)	C(3)-C(4)-Fe(1)	69.83(9)
C(8)-C(9)	1.419(2)	C(2)-Fe(1)-C(4)	68.56(7)	C(5)-C(4)-Fe(1)	67.76(9)
C(9)-C(10)	1.427(2)	C(5)-Fe(1)-C(4)	40.77(6)	C(4)-C(5)-C(1)	108.07(15)
C(11)-C(12)	1.622(3)	C(7)-Fe(1)-C(4)	125.69(7)	C(4)-C(5)-Fe(1)	71.46(9)
C(11')-C(12)	1.664(5)	C(3)-Fe(1)-C(4)	40.01(7)	C(1)-C(5)-Fe(1)	66.55(9)
C(12)-C(15')	1.320(6)	C(9)-Fe(1)-C(4)	139.23(6)	C(7)-C(6)-C(10)	105.14(12)
C(12)-C(14)	1.403(4)	C(1)-Fe(1)-C(8)	150.47(6)	C(7)-C(6)-B(1)	126.29(13)
C(12)-C(13)	1.522(2)	C(6)-Fe(1)-C(8)	70.65(6)	C(10)-C(6)-B(1)	125.69(13)
C(12)-C(15)	1.586(3)	C(10)-Fe(1)-C(8)	68.61(6)	C(7)-C(6)-Fe(1)	70.15(8)
C(12)-C(14')	1.730(6)	C(2)-Fe(1)-C(8)	163.13(7)	C(10)-C(6)-Fe(1)	69.68(8)
C(16)-C(18)	1.522(2)	C(5)-Fe(1)-C(8)	127.11(7)	B(1)-C(6)-Fe(1)	109.60(9)
C(16)-C(17)	1.523(2)	C(7)-Fe(1)-C(8)	40.90(6)	C(8)-C(7)-C(6)	109.54(13)
C(19)-C(21)	1.519(3)	C(3)-Fe(1)-C(8)	137.63(6)	C(8)-C(7)-Fe(1)	71.25(8)
C(19)-C(20)	1.529(3)	C(9)-Fe(1)-C(8)	40.18(7)	C(6)-C(7)-Fe(1)	67.70(8)
		C(4)-Fe(1)-C(8)	121.77(6)	C(9)-C(8)-C(7)	107.90(13)
C(1)-Fe(1)-C(6)	86.35(6)	C(1)-N(1)-B(1)	114.3(3)	C(9)-C(8)-Fe(1)	69.83(9)
C(1)-Fe(1)-C(10)	106.62(6)	C(1)-N(1)-C(11)	114.7(3)	C(7)-C(8)-Fe(1)	67.85(8)
C(6)-Fe(1)-C(10)	42.36(6)	B(1)-N(1)-C(11)	129.0(3)	C(8)-C(9)-C(10)	107.75(13)
C(1)-Fe(1)-C(2)	42.19(7)	C(1)-N(1')-C(11')	116.5(5)	C(8)-C(9)-Fe(1)	69.99(9)
C(6)-Fe(1)-C(2)	108.22(6)	C(1)-N(1')-B(1)	108.9(4)	C(10)-C(9)-Fe(1)	67.53(8)
C(10)-Fe(1)-C(2)	98.85(7)	C(11')-N(1')-B(1)	134.5(5)	C(9)-C(10)-C(6)	109.63(14)
C(1)-Fe(1)-C(5)	42.08(7)	B(1)-N(2)-C(19)	122.80(12)	C(9)-C(10)-Fe(1)	71.51(9)
C(6)-Fe(1)-C(5)	107.17(6)	B(1)-N(2)-C(16)	124.02(12)	C(6)-C(10)-Fe(1)	67.96(8)
C(10)-Fe(1)-C(5)	144.06(6)	C(19)-N(2)-C(16)	113.16(11)	N(1)-C(11)-C(12)	115.1(2)
C(2)-Fe(1)-C(5)	69.67(7)	N(2)-B(1)-N(1)	125.87(19)	N(1')-C(11')-C(12)	111.0(4)
C(1)-Fe(1)-C(7)	109.60(6)	N(2)-B(1)-N(1')	122.8(3)	C(15')-C(12)-C(13)	124.0(3)
C(6)-Fe(1)-C(7)	42.16(6)	N(2)-B(1)-C(6)	121.85(13)	C(14)-C(12)-C(13)	115.1(2)
C(10)-Fe(1)-C(7)	69.30(6)	N(1)-B(1)-C(6)	111.87(18)	C(14)-C(12)-C(15)	112.6(2)
C(2)-Fe(1)-C(7)	146.74(6)	N(1')-B(1)-C(6)	113.2(3)	C(13)-C(12)-C(15)	103.63(16)
C(5)-Fe(1)-C(7)	101.19(7)	C(5)-C(1)-C(2)	107.47(13)	C(14)-C(12)-C(11)	114.94(18)
C(1)-Fe(1)-C(3)	70.01(6)	C(5)-C(1)-N(1)	132.60(18)	C(13)-C(12)-C(11)	108.86(15)
C(6)-Fe(1)-C(3)	148.98(6)	C(2)-C(1)-N(1)	119.13(18)	C(15)-C(12)-C(11)	100.05(18)
C(10)-Fe(1)-C(3)	125.02(7)	C(5)-C(1)-N(1')	111.0(3)	C(15')-C(12)-C(11')	117.5(3)
C(2)-Fe(1)-C(3)	40.82(6)	C(2)-C(1)-N(1')	141.1(3)	C(13)-C(12)-C(11')	104.60(19)
C(5)-Fe(1)-C(3)	68.47(7)	C(5)-C(1)-Fe(1)	71.36(9)	C(15')-C(12)-C(14')	109.3(4)
C(7)-Fe(1)-C(3)	165.57(7)	C(2)-C(1)-Fe(1)	71.15(9)	C(13)-C(12)-C(14')	103.1(2)
C(1)-Fe(1)-C(9)	147.23(7)	N(1)-C(1)-Fe(1)	114.77(17)	C(11')-C(12)-C(14')	93.1(3)
C(6)-Fe(1)-C(9)	70.77(6)	N(1')-C(1)-Fe(1)	116.7(3)	N(2)-C(16)-C(18)	112.67(13)
C(10)-Fe(1)-C(9)	40.97(6)	C(3)-C(2)-C(1)	107.92(15)	N(2)-C(16)-C(17)	114.06(12)
C(2)-Fe(1)-C(9)	123.03(7)	C(3)-C(2)-Fe(1)	71.43(9)	C(18)-C(16)-C(17)	111.30(14)
C(5)-Fe(1)-C(9)	167.29(7)	C(1)-C(2)-Fe(1)	66.66(8)	N(2)-C(19)-C(21)	112.87(15)
C(7)-Fe(1)-C(9)	68.59(6)	C(4)-C(3)-C(2)	108.37(14)	N(2)-C(19)-C(20)	112.23(15)
C(3)-Fe(1)-C(9)	120.01(7)	C(4)-C(3)-Fe(1)	70.16(9)	C(21)-C(19)-C(20)	111.80(15)
C(1)-Fe(1)-C(4)	69.98(6)	C(2)-C(3)-Fe(1)	67.75(8)		
C(6)-Fe(1)-C(4)	147.78(6)	C(3)-C(4)-C(5)	108.09(14)		

Table S4. Bond Lengths (Å) and Bond Angles (deg) for Compound **2c**.

Fe(1)-C(1)	1.9474(16)	Si(1)-C(16)	1.9233(16)	B(1)-C(16)	1.624(2)
Fe(1)-C(6)	1.9859(16)	Si(2)-C(21)	1.8816(19)	C(1)-C(5)	1.428(2)
Fe(1)-C(7)	2.0103(19)	Si(2)-C(22)	1.8837(18)	C(1)-C(2)	1.434(2)
Fe(1)-C(2)	2.0105(18)	Si(2)-C(20)	1.9014(19)	C(2)-C(3)	1.426(2)
Fe(1)-C(10)	2.0149(17)	Si(2)-C(16)	1.9319(15)	C(3)-C(4)	1.418(3)
Fe(1)-C(5)	2.0215(17)	Si(3)-C(25)	1.8762(18)	C(4)-C(5)	1.422(3)
Fe(1)-C(8)	2.0698(19)	Si(3)-C(24)	1.8814(17)	C(6)-C(7)	1.442(2)
Fe(1)-C(9)	2.0710(18)	Si(3)-C(23)	1.8867(19)	C(6)-C(10)	1.443(2)
Fe(1)-C(3)	2.0713(18)	Si(3)-C(16)	1.9250(16)	C(7)-C(8)	1.426(3)
Fe(1)-C(4)	2.0769(17)	N(1)-B(1)	1.436(2)	C(8)-C(9)	1.421(3)
Si(1)-C(19)	1.8811(18)	N(1)-C(1)	1.446(2)	C(9)-C(10)	1.428(3)
Si(1)-C(17)	1.8828(19)	N(1)-C(11)	1.473(2)	C(11)-C(12)	1.547(2)
Si(1)-C(18)	1.8865(19)	B(1)-C(6)	1.614(2)	C(12)-C(14)	1.532(2)

C(12)-C(15)	1.536(2)
C(12)-C(13)	1.539(2)
C(1)-Fe(1)-C(6)	85.64(7)
C(1)-Fe(1)-C(7)	106.86(7)
C(6)-Fe(1)-C(7)	42.29(7)
C(1)-Fe(1)-C(2)	42.43(7)
C(6)-Fe(1)-C(2)	106.62(7)
C(7)-Fe(1)-C(2)	144.20(7)
C(1)-Fe(1)-C(10)	108.22(7)
C(6)-Fe(1)-C(10)	42.26(7)
C(7)-Fe(1)-C(10)	69.38(8)
C(2)-Fe(1)-C(10)	99.63(7)
C(1)-Fe(1)-C(5)	42.11(6)
C(6)-Fe(1)-C(5)	107.59(7)
C(7)-Fe(1)-C(5)	99.41(8)
C(2)-Fe(1)-C(5)	70.00(7)
C(10)-Fe(1)-C(5)	145.61(7)
C(1)-Fe(1)-C(8)	147.53(8)
C(6)-Fe(1)-C(8)	70.68(7)
C(7)-Fe(1)-C(8)	40.87(7)
C(2)-Fe(1)-C(8)	165.73(8)
C(10)-Fe(1)-C(8)	68.68(8)
C(5)-Fe(1)-C(8)	124.27(8)
C(1)-Fe(1)-C(9)	149.04(7)
C(6)-Fe(1)-C(9)	70.52(7)
C(7)-Fe(1)-C(9)	68.45(8)
C(2)-Fe(1)-C(9)	125.58(8)
C(10)-Fe(1)-C(9)	40.87(7)
C(5)-Fe(1)-C(9)	164.41(8)
C(8)-Fe(1)-C(9)	40.15(8)
C(1)-Fe(1)-C(3)	70.04(7)
C(6)-Fe(1)-C(3)	147.38(7)
C(7)-Fe(1)-C(3)	165.53(8)
C(2)-Fe(1)-C(3)	40.85(7)
C(10)-Fe(1)-C(3)	125.09(8)
C(5)-Fe(1)-C(3)	68.54(8)
C(8)-Fe(1)-C(3)	139.57(8)
C(9)-Fe(1)-C(3)	121.74(8)
C(1)-Fe(1)-C(4)	69.70(7)
C(6)-Fe(1)-C(4)	148.12(7)

C(7)-Fe(1)-C(4)	125.55(8)
C(2)-Fe(1)-C(4)	68.55(7)
C(10)-Fe(1)-C(4)	165.07(8)
C(5)-Fe(1)-C(4)	40.57(7)
C(8)-Fe(1)-C(4)	121.39(8)
C(9)-Fe(1)-C(4)	139.04(8)
C(3)-Fe(1)-C(4)	39.99(8)
C(19)-Si(1)-C(17)	104.32(9)
C(19)-Si(1)-C(18)	107.55(9)
C(17)-Si(1)-C(18)	100.63(9)
C(19)-Si(1)-C(16)	109.17(8)
C(17)-Si(1)-C(16)	115.71(8)
C(18)-Si(1)-C(16)	118.26(8)
C(21)-Si(2)-C(22)	105.87(9)
C(21)-Si(2)-C(20)	104.67(9)
C(22)-Si(2)-C(20)	103.57(9)
C(21)-Si(2)-C(16)	113.00(7)
C(22)-Si(2)-C(16)	113.87(8)
C(20)-Si(2)-C(16)	114.84(8)
C(25)-Si(3)-C(24)	106.02(8)
C(25)-Si(3)-C(23)	106.96(9)
C(24)-Si(3)-C(23)	100.14(9)
C(25)-Si(3)-C(16)	108.74(8)
C(24)-Si(3)-C(16)	115.19(8)
C(23)-Si(3)-C(16)	118.77(8)
B(1)-N(1)-C(1)	116.77(13)
B(1)-N(1)-C(11)	126.78(13)
C(1)-N(1)-C(11)	114.95(12)
N(1)-B(1)-C(6)	110.98(14)
N(1)-B(1)-C(16)	125.70(15)
C(6)-B(1)-C(16)	123.31(13)
C(5)-C(1)-C(2)	107.86(15)
C(5)-C(1)-N(1)	125.49(15)
C(2)-C(1)-N(1)	126.00(14)
C(5)-C(1)-Fe(1)	71.72(9)
C(2)-C(1)-Fe(1)	71.14(9)
N(1)-C(1)-Fe(1)	115.64(10)
C(3)-C(2)-C(1)	107.67(16)
C(3)-C(2)-Fe(1)	71.87(11)
C(1)-C(2)-Fe(1)	66.43(9)
C(4)-C(3)-C(2)	108.11(16)

C(4)-C(3)-Fe(1)	70.22(11)
C(2)-C(3)-Fe(1)	67.28(10)
C(3)-C(4)-C(5)	108.50(16)
C(3)-C(4)-Fe(1)	69.79(10)
C(5)-C(4)-Fe(1)	67.62(9)
C(4)-C(5)-C(1)	107.79(16)
C(4)-C(5)-Fe(1)	71.81(10)
C(1)-C(5)-Fe(1)	66.17(9)
C(7)-C(6)-C(10)	105.17(15)
C(7)-C(6)-B(1)	124.25(15)
C(10)-C(6)-B(1)	128.15(15)
C(7)-C(6)-Fe(1)	69.76(10)
C(10)-C(6)-Fe(1)	69.94(9)
B(1)-C(6)-Fe(1)	110.96(10)
C(8)-C(7)-C(6)	109.86(17)
C(8)-C(7)-Fe(1)	71.80(11)
C(6)-C(7)-Fe(1)	67.95(10)
C(9)-C(8)-C(7)	107.50(17)
C(9)-C(8)-Fe(1)	69.97(11)
C(7)-C(8)-Fe(1)	67.32(10)
C(8)-C(9)-C(10)	107.99(17)
C(8)-C(9)-Fe(1)	69.88(11)
C(10)-C(9)-Fe(1)	67.45(10)
C(9)-C(10)-C(6)	109.45(17)
C(9)-C(10)-Fe(1)	71.68(10)
C(6)-C(10)-Fe(1)	67.79(9)
N(1)-C(11)-C(12)	119.99(14)
C(14)-C(12)-C(15)	110.18(14)
C(14)-C(12)-C(13)	108.66(15)
C(15)-C(12)-C(13)	107.14(15)
C(14)-C(12)-C(11)	112.31(13)
C(15)-C(12)-C(11)	112.44(14)
C(13)-C(12)-C(11)	105.82(14)
B(1)-C(16)-Si(1)	109.28(10)
B(1)-C(16)-Si(3)	106.24(10)
Si(1)-C(16)-Si(3)	119.04(8)
B(1)-C(16)-Si(2)	109.00(11)
Si(1)-C(16)-Si(2)	106.75(8)
Si(3)-C(16)-Si(2)	106.21(7)

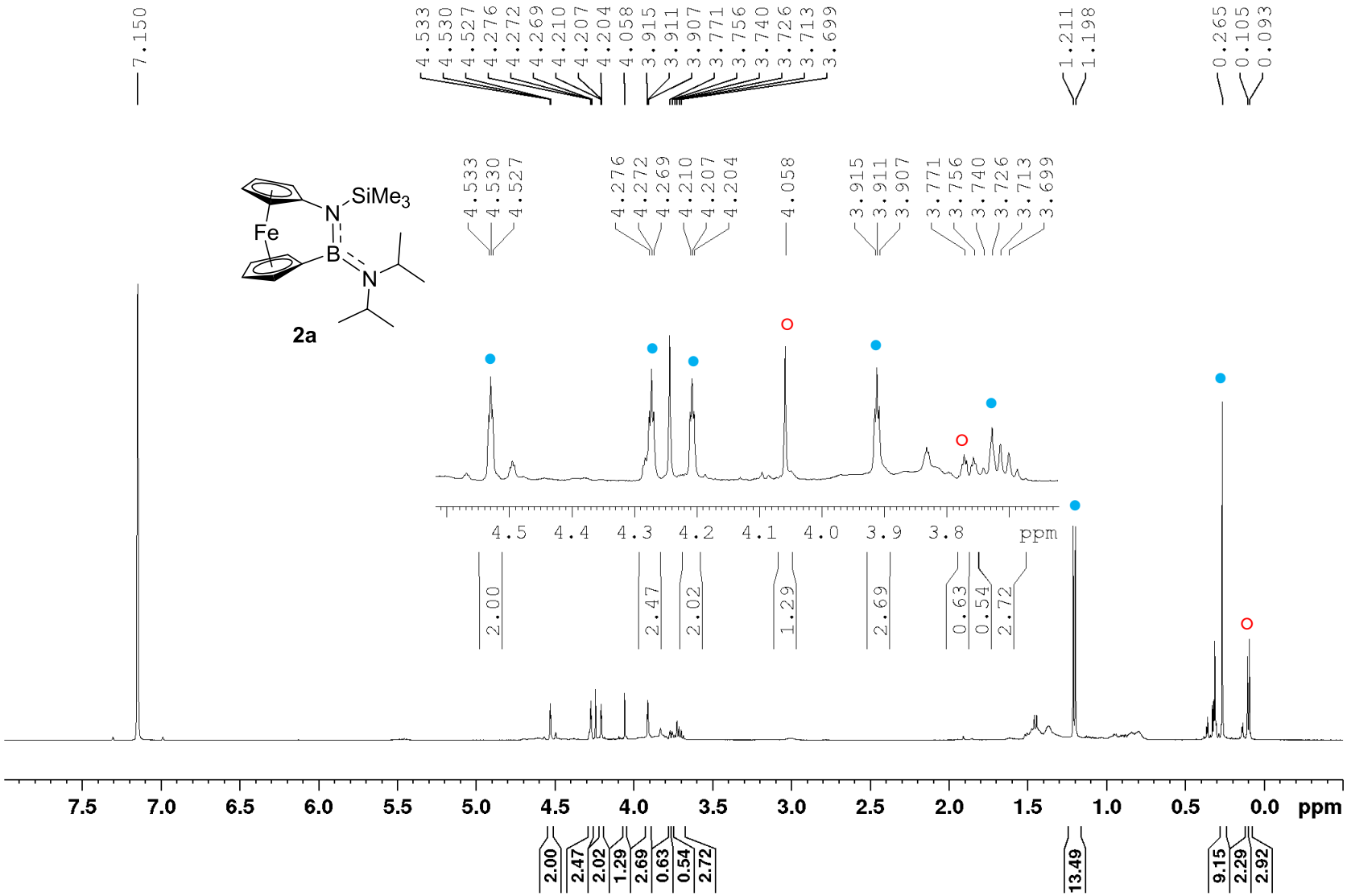

Figure S1. ^{1}H NMR (500.3 MHz) spectrum of **2a** in C_6D_6, taken from an aliquot of the reaction mixture 1 h after the addition of the dichloride. The peaks marked with ● resulted from the targeted compound, and the peaks marked with ○ could be assigned to the known (trimethylsilylamino)ferrocene (for the latter assignement see ref. [3]).

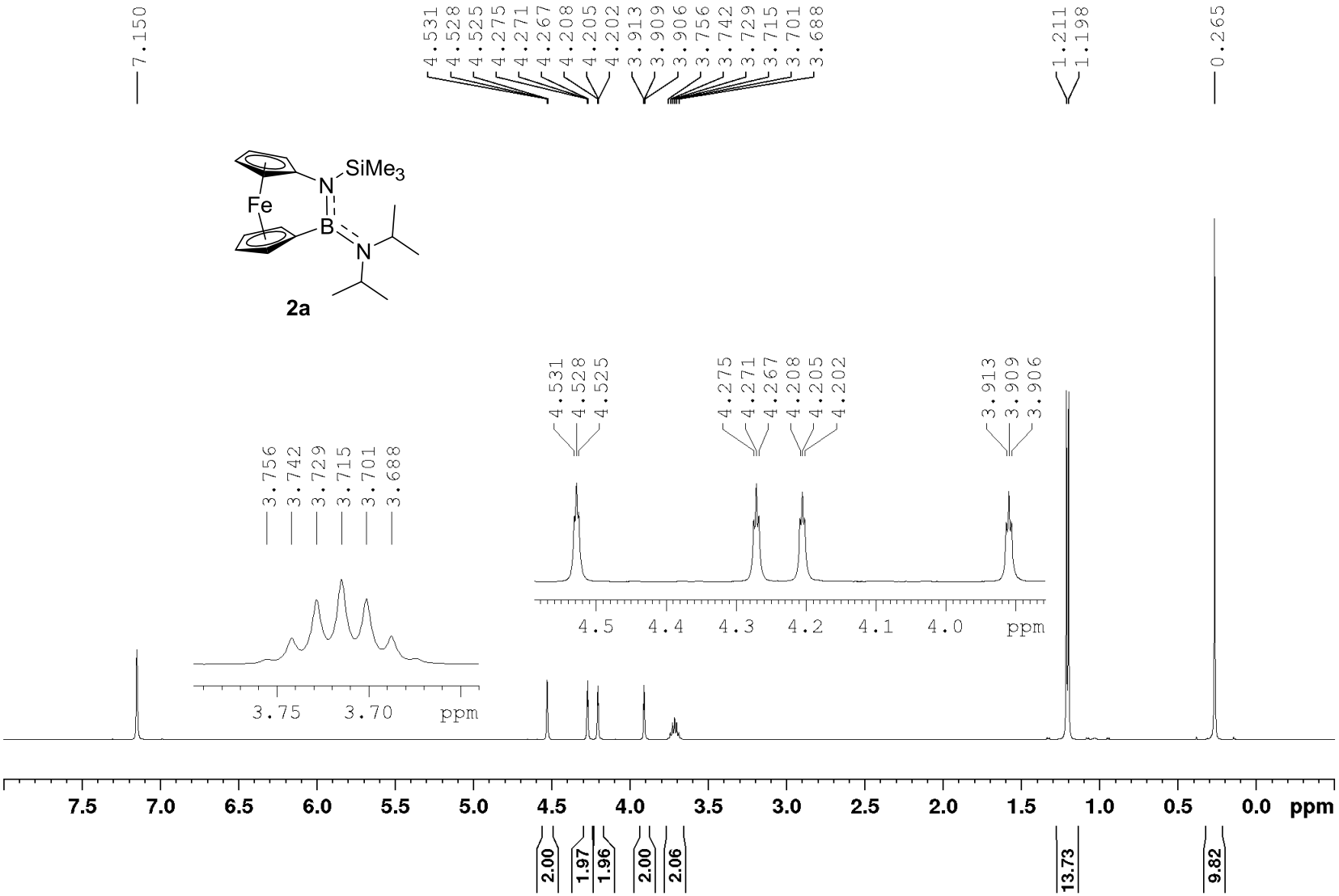

Figure S2. ^{1}H NMR (500.1 MHz) spectrum of **2a** in C_6D_6.

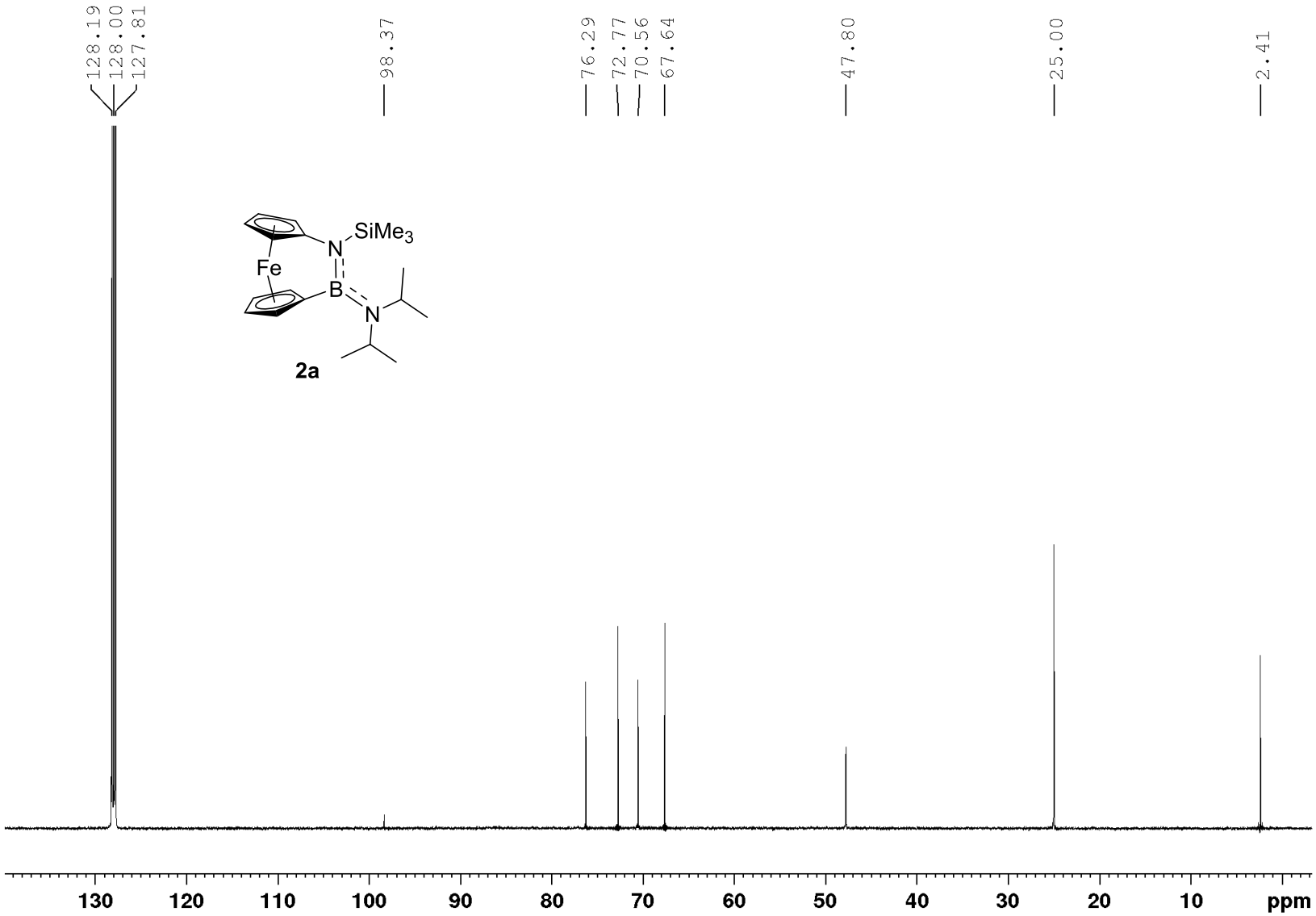

Figure S3. $^{13}C\{^{1}H\}$ NMR (125.8 MHz) spectrum of **2a** in C_6D_6.

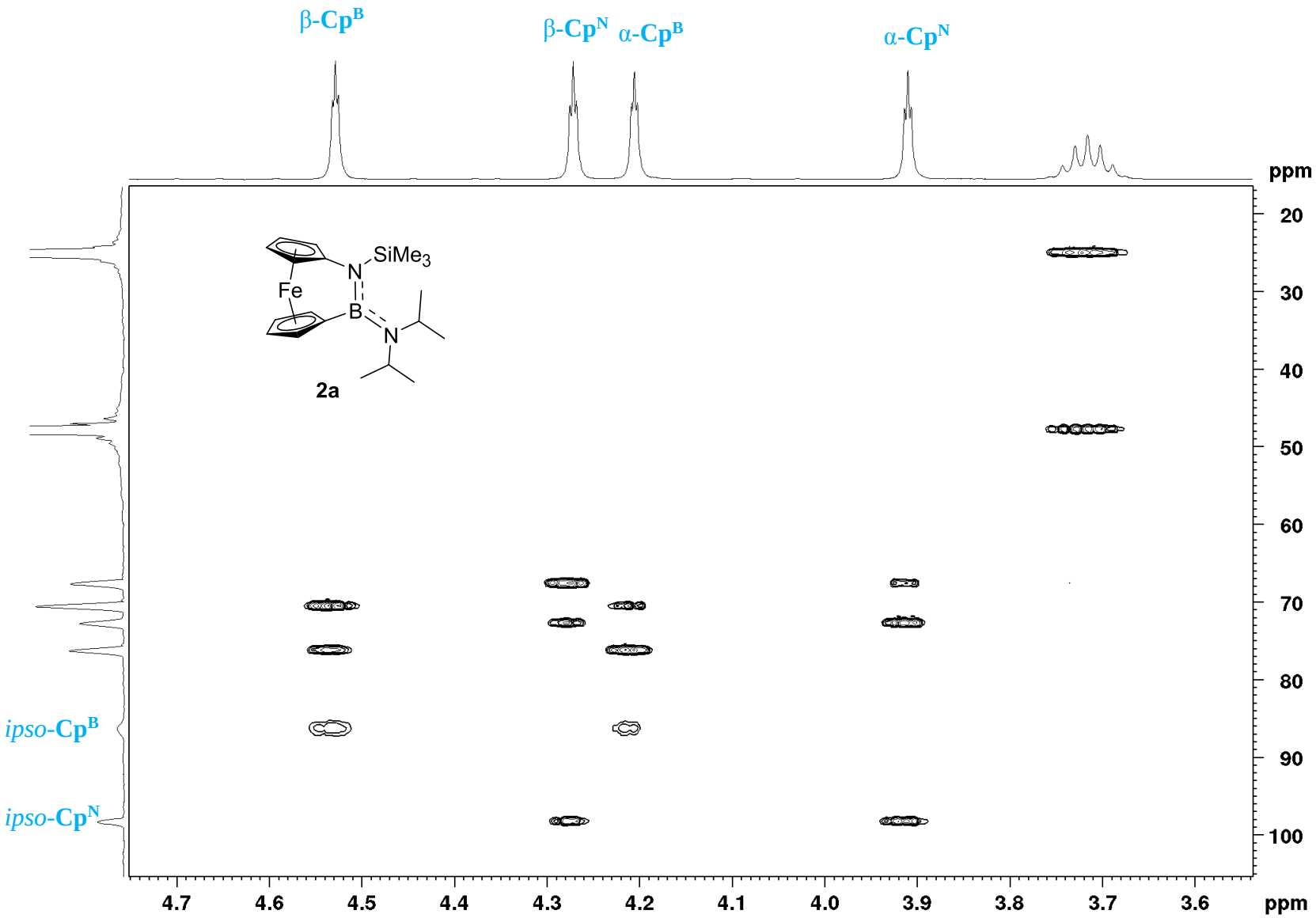

Figure S4. ^{1}H-^{13}C HMBC spectrum of **2a** in C_6D_6 (selected area).

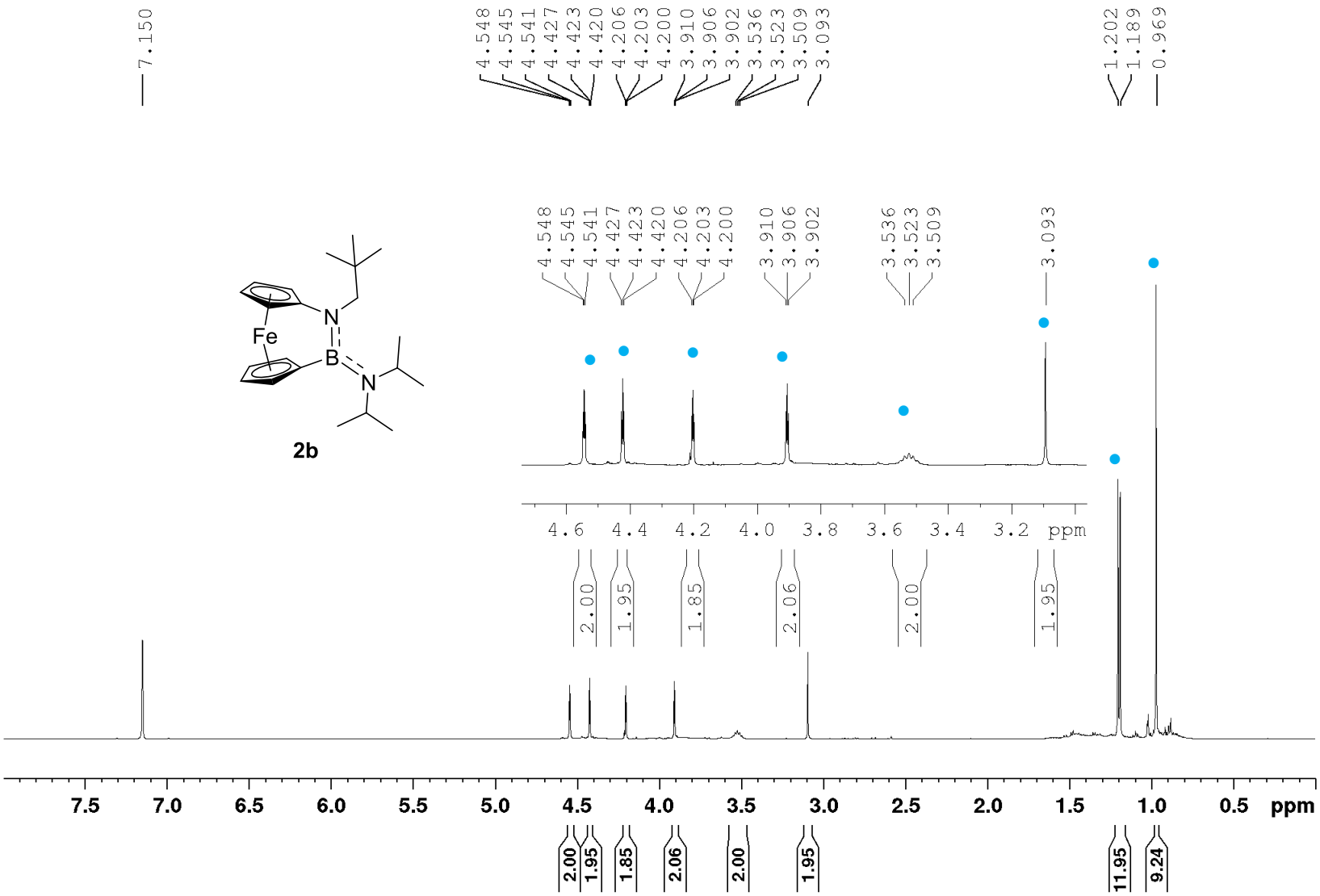

Figure S5. ^{1}H NMR (500.3 MHz) spectrum of **2b** in C_6D_6, taken from an aliquot of the reaction mixture 1 h after the addition of the dichloride. The peaks marked with ● resulted from the targeted compound.

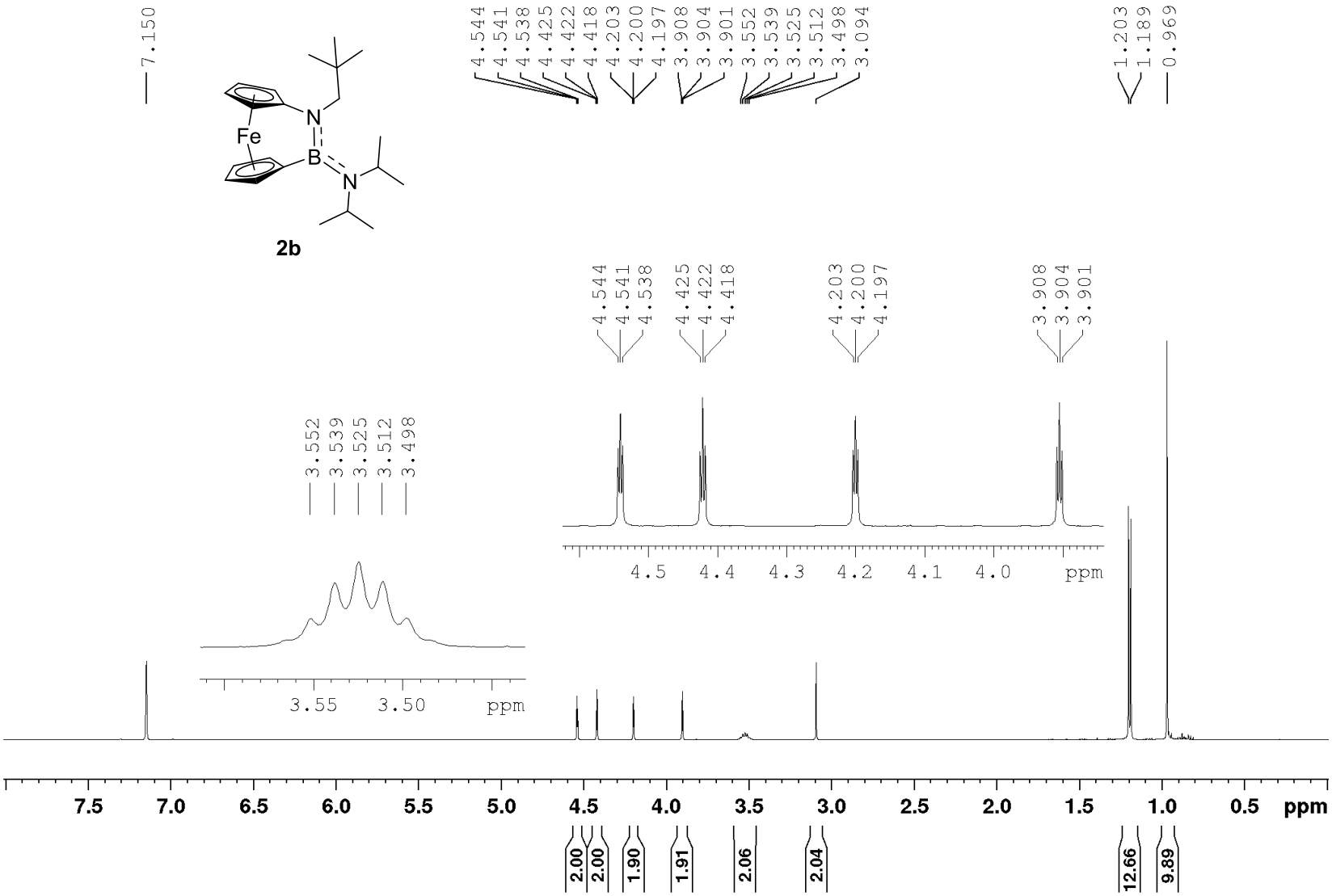

Figure S6. ^{1}H NMR (500.3 MHz) spectrum of **2b** in C_6D_6.

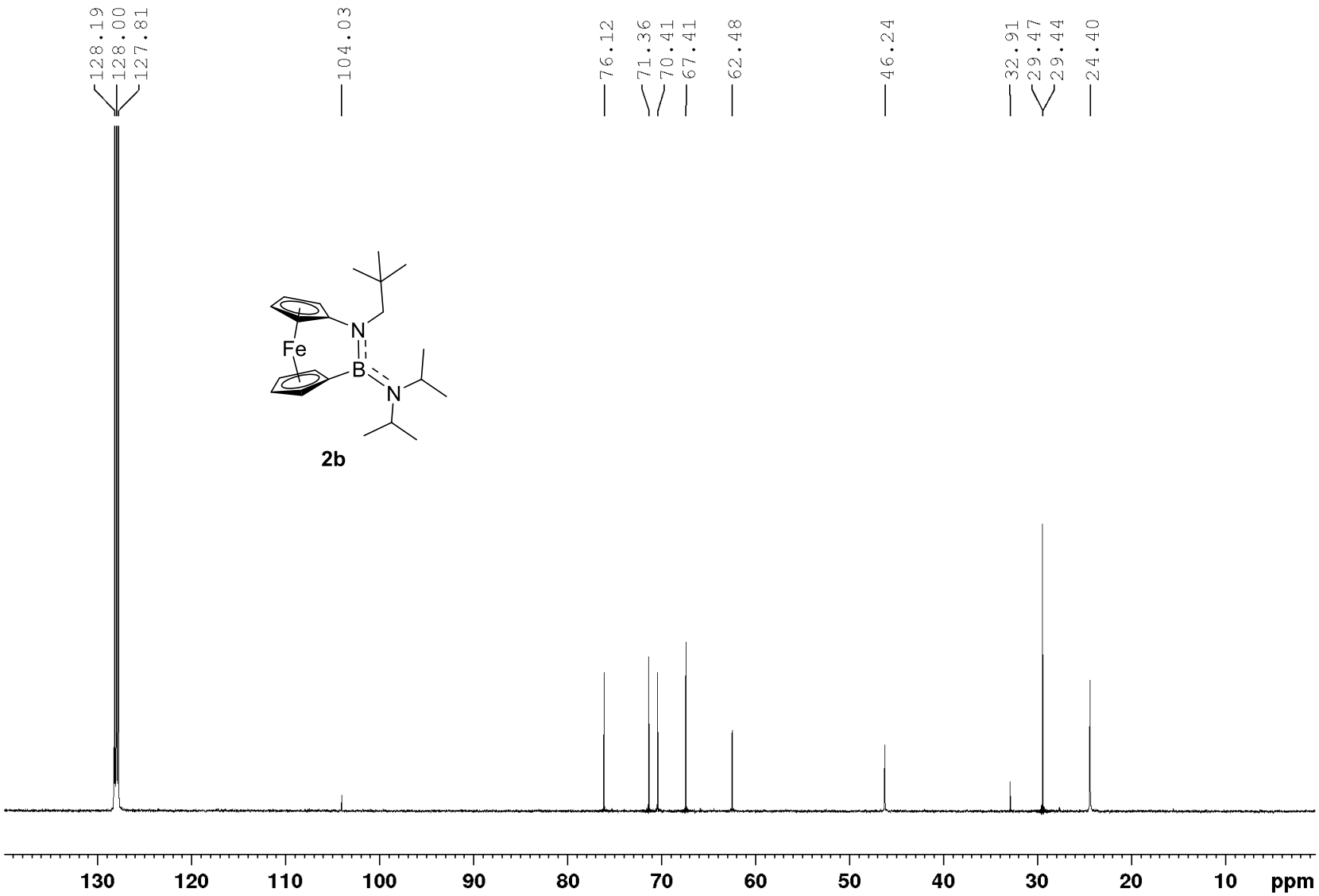

Figure S7. $^{13}C\{^{1}H\}$ NMR (125.8 MHz) spectrum of **2b** in C_6D_6.

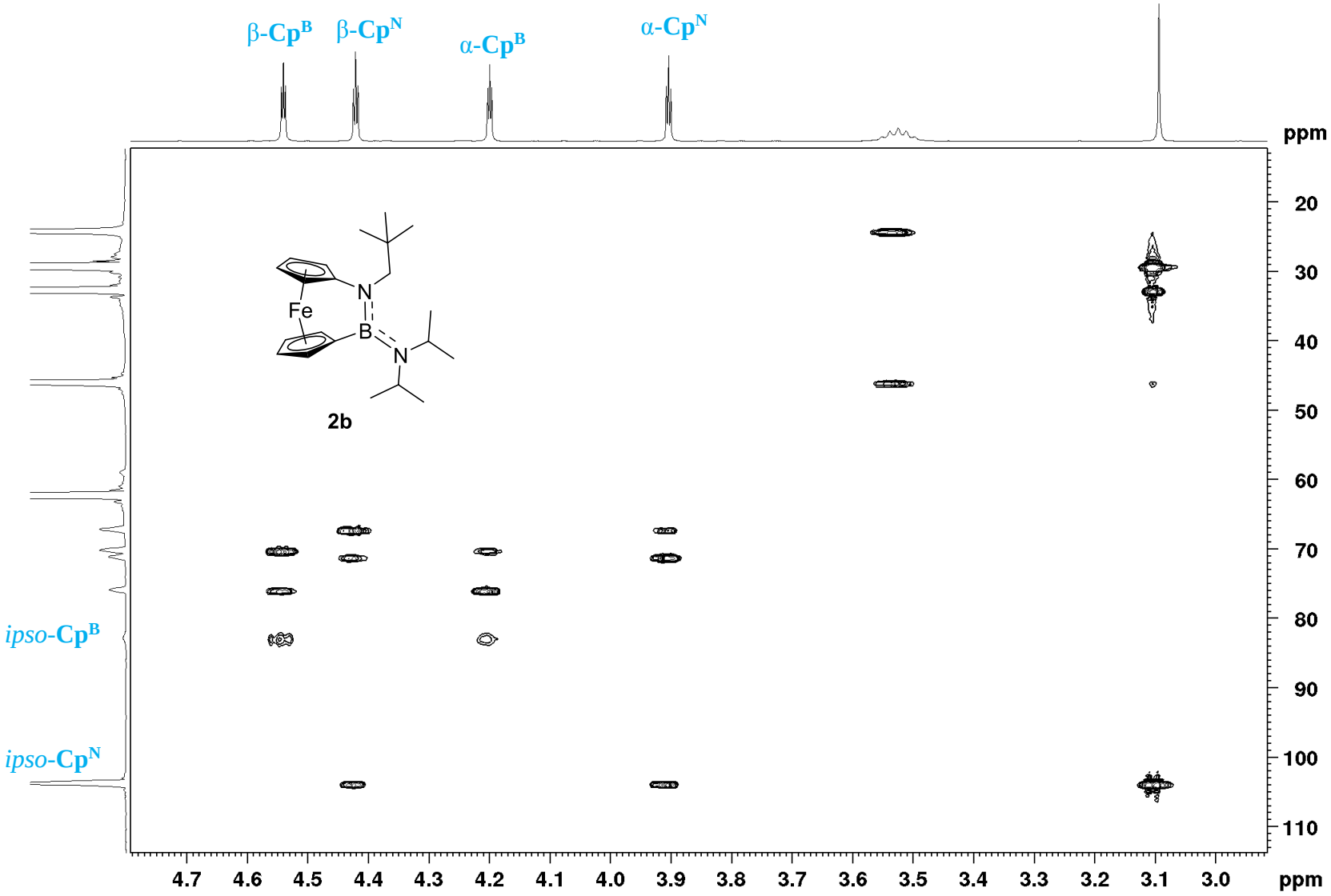

Figure S8. ^{1}H-^{13}C HMBC spectrum of **2b** in C_6D_6 (selected area).

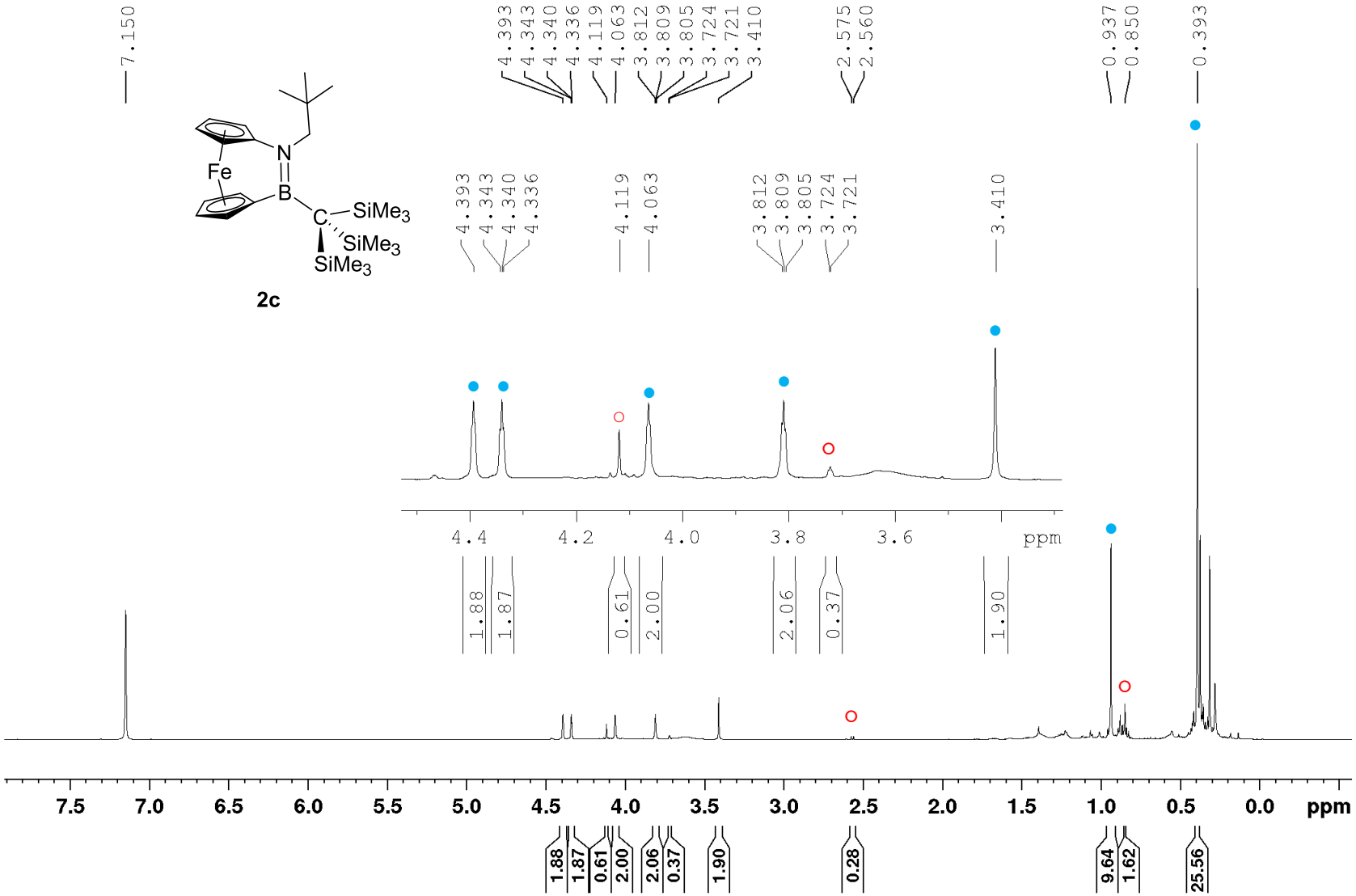

Figure S9. ^{1}H NMR (500.1 MHz) spectrum of **2c** in C_6D_6, taken from an aliquot of the reaction mixture 1 h after the addition of the dichloride. The peaks marked with ● resulted from the targeted compound, and the peaks marked with ○ could be assigned to the known (neopentylamino)ferrocene (for the latter assignement see ref [4]).

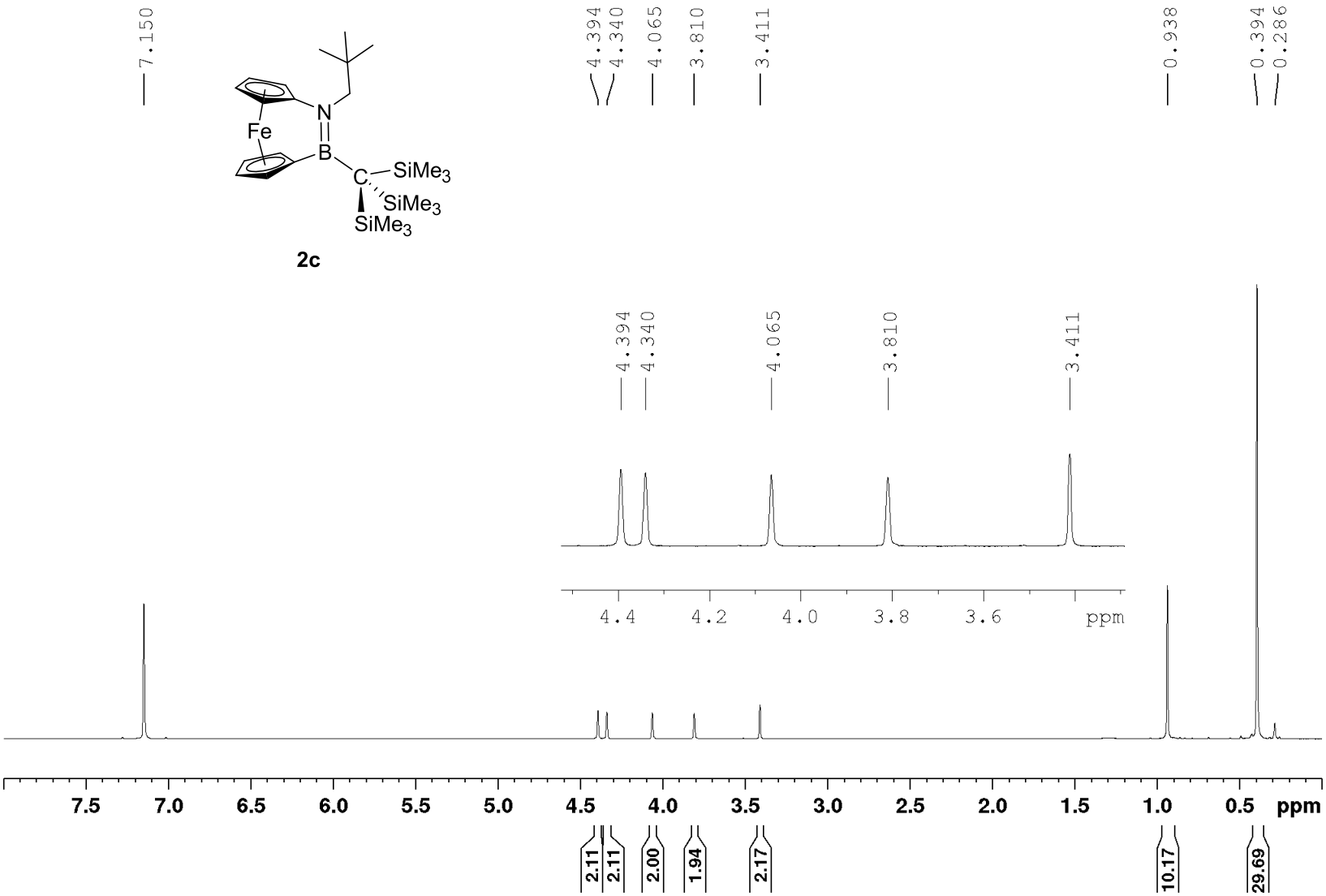

Figure S10. ^{1}H NMR (600.2 MHz) spectrum of **2c** in C_6D_6.

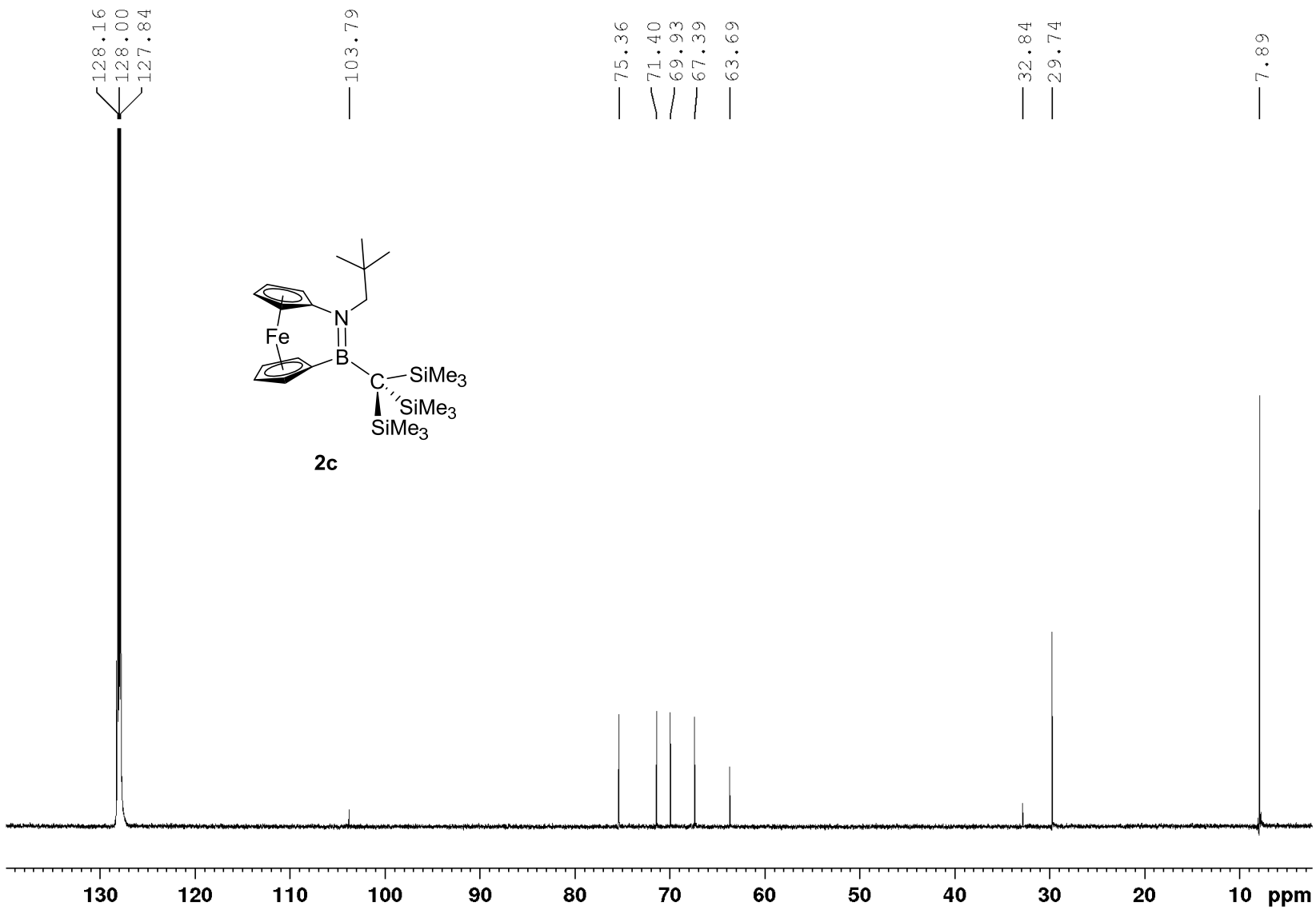

Figure S11. $^{13}C\{^{1}H\}$ NMR (150.9 MHz) spectrum of **2c** in C_6D_6.

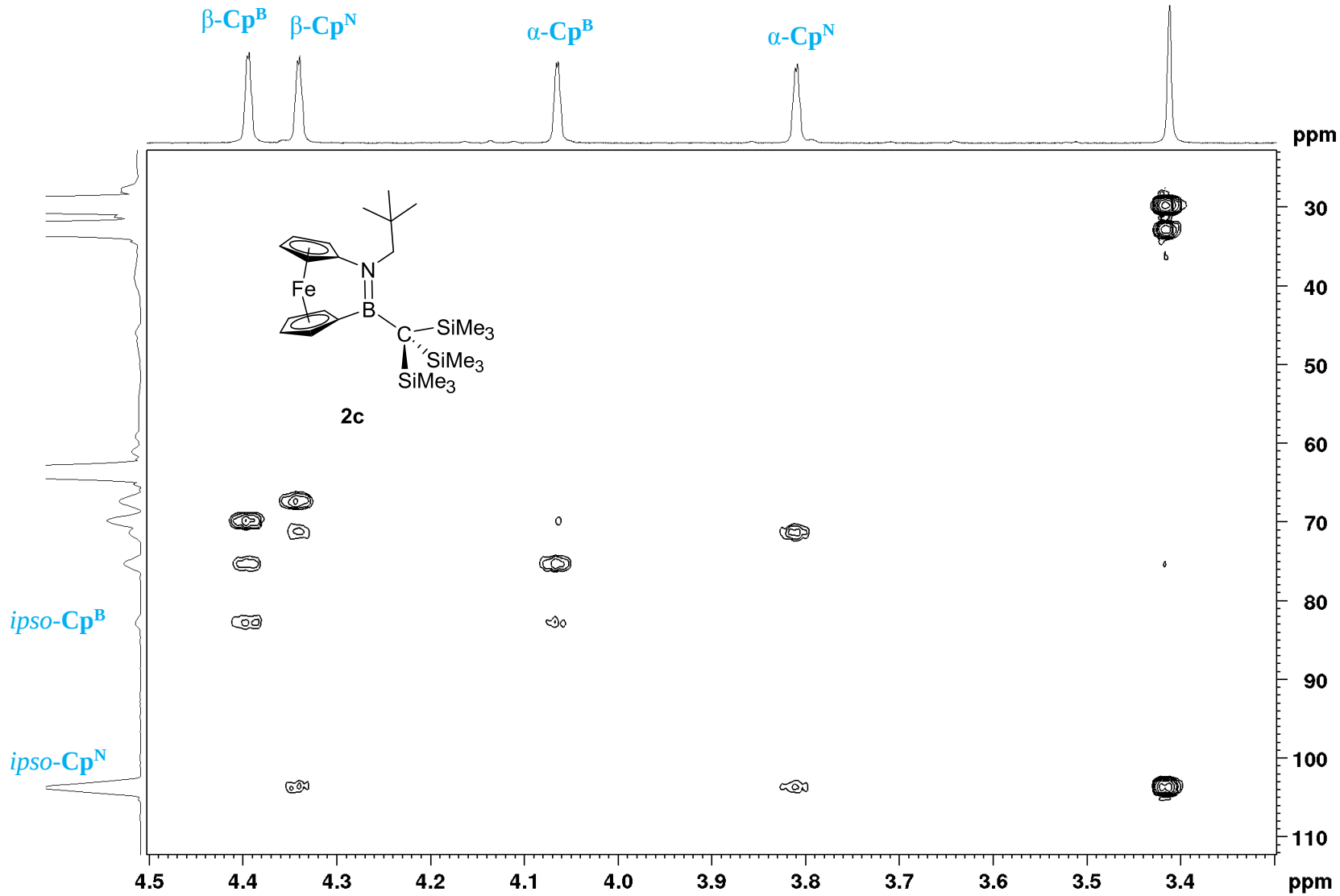

Figure S12. ^{1}H-^{13}C HMBC spectrum of **2c** in C_6D_6 (selected area).

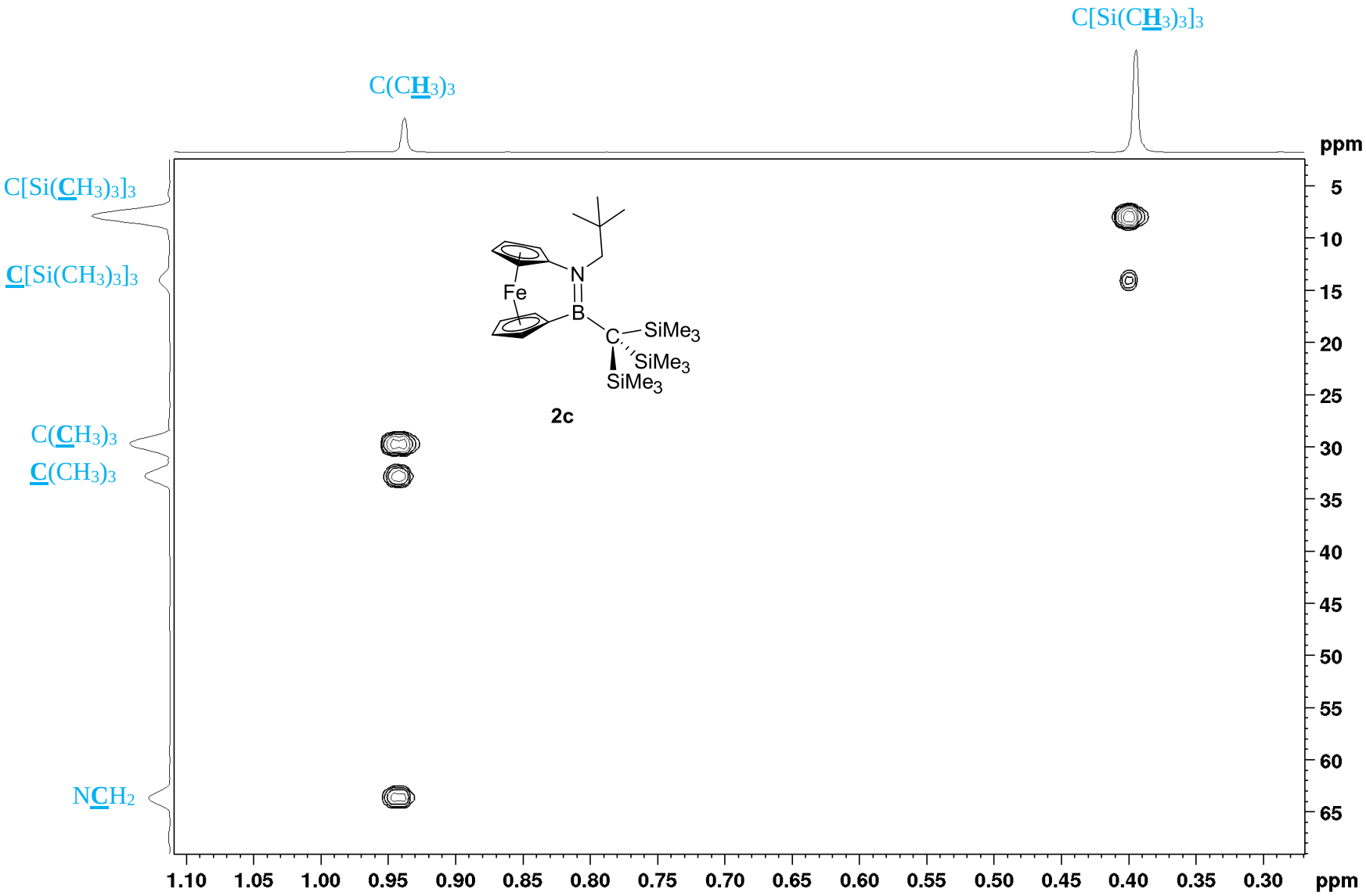

Figure S13. ^{1}H-^{13}C HMBC spectrum of **2c** in C_6D_6 (selected area).

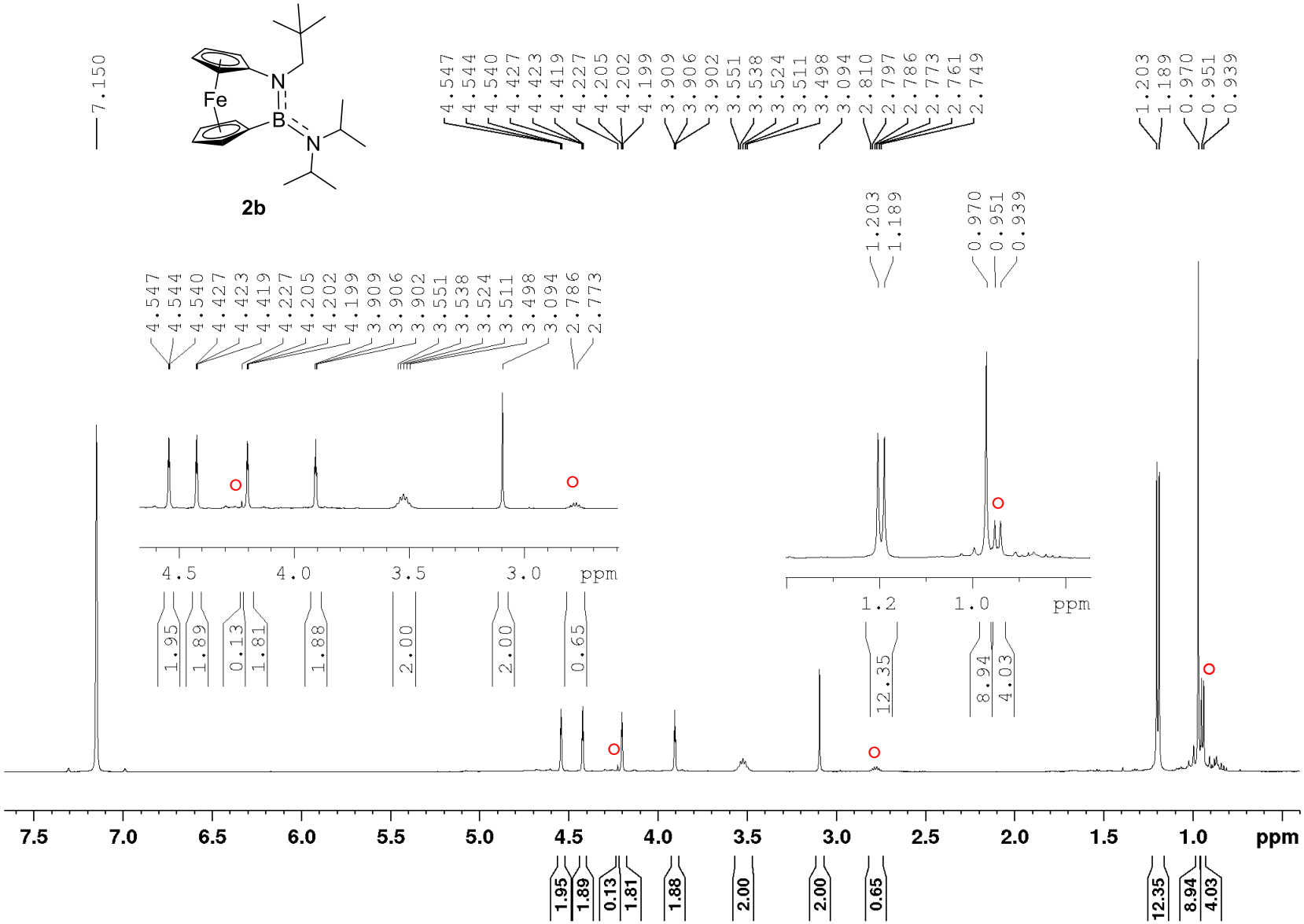

Figure S14. ^{1}H NMR (500.3 MHz) spectrum after the TROP experiment of **2b** in C_6D_6 (after 4 h at 300 ºC; see Experimental Section on page S4). New signals are marked with ○.

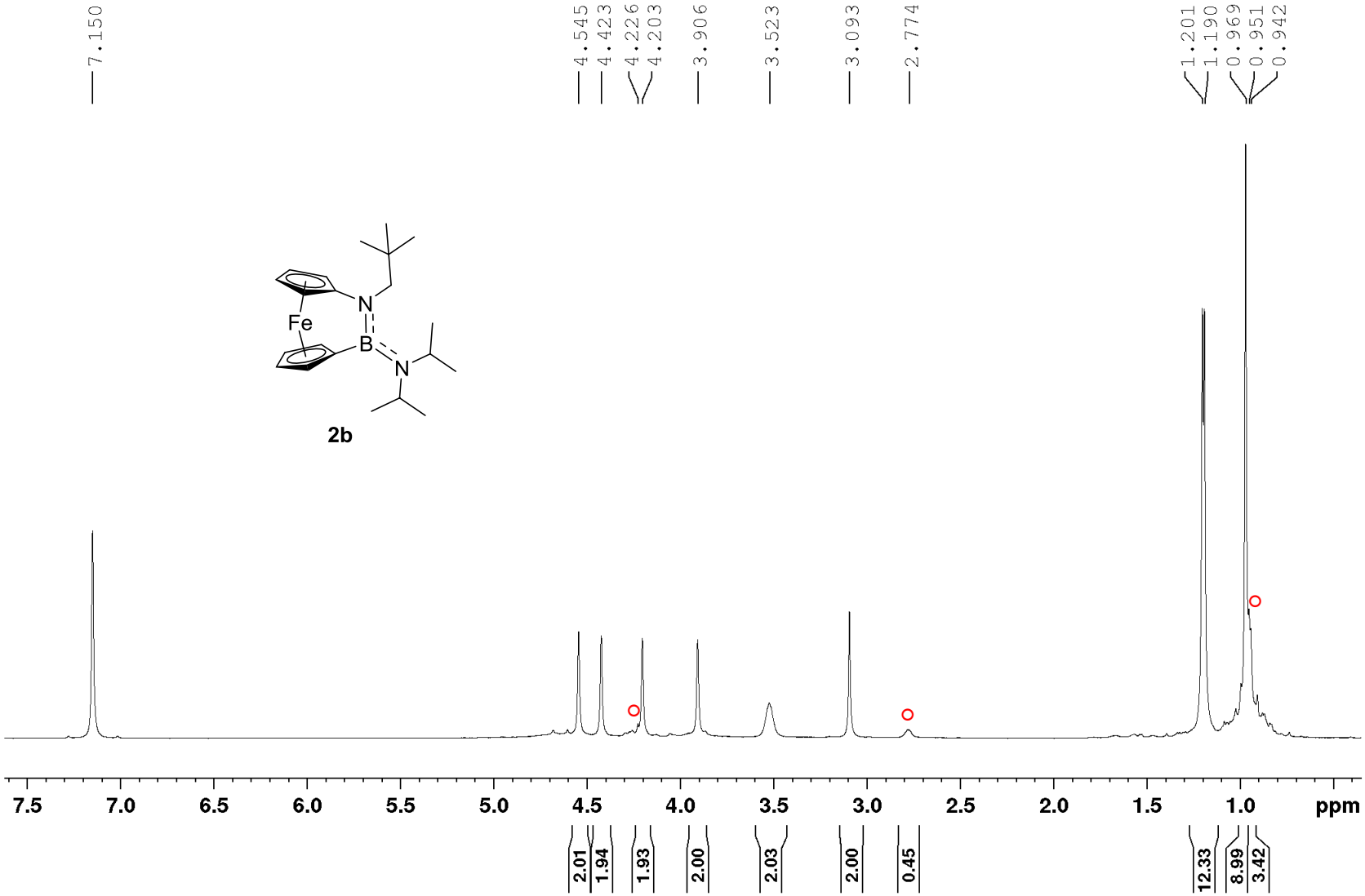

Figure S15. ^{1}H NMR (600.2 MHz) spectrum after the TROP experiment of **2b** in C_6D_6 (after 22 h at 300 ºC; see Experimental Section on page S4). New signals are marked with ○.

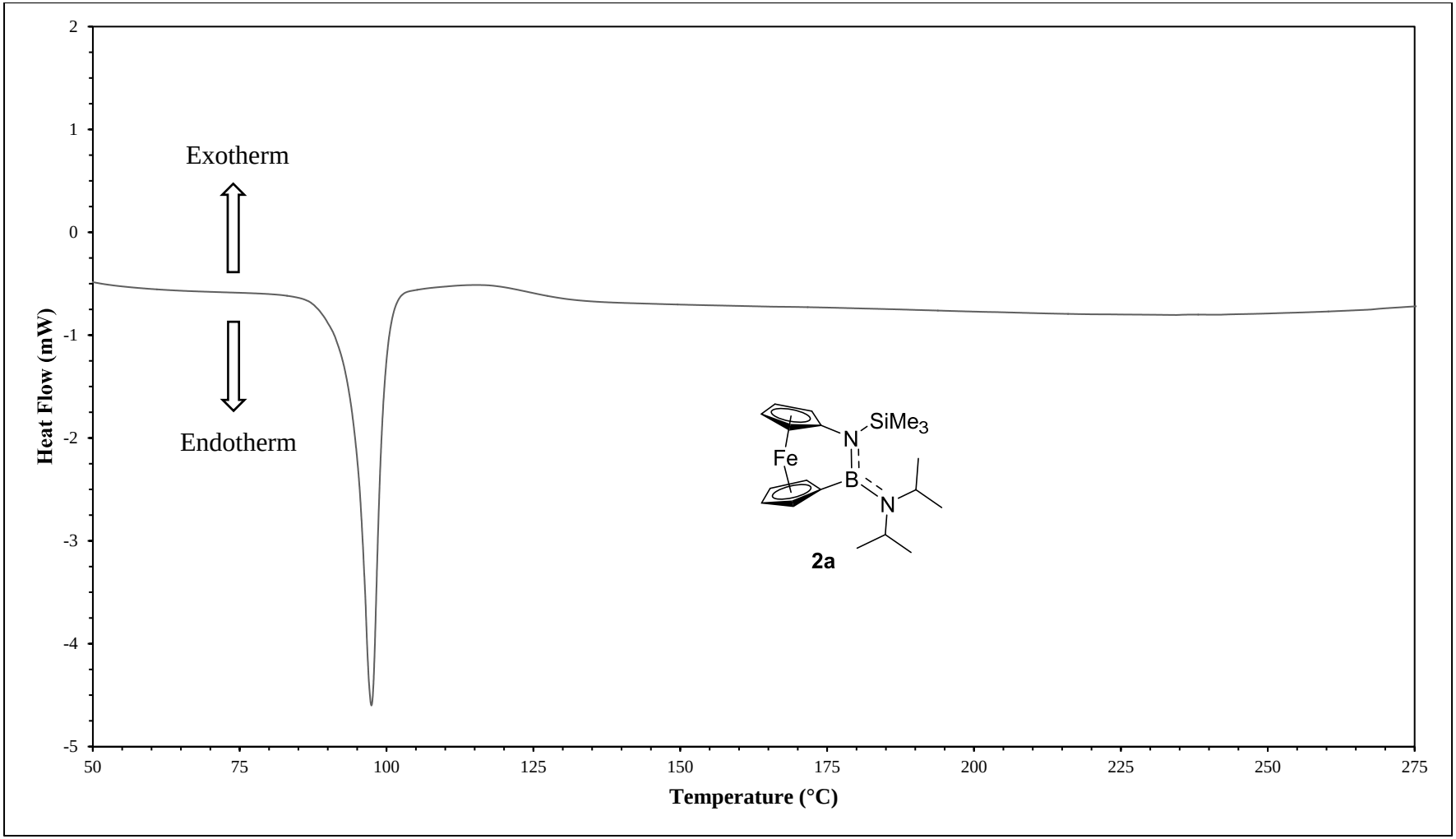

Figure S16. DSC thermogram of **2a**. Heating rate of 10 °C min^{-1}, melting endotherm at T (max) = 97 °C.

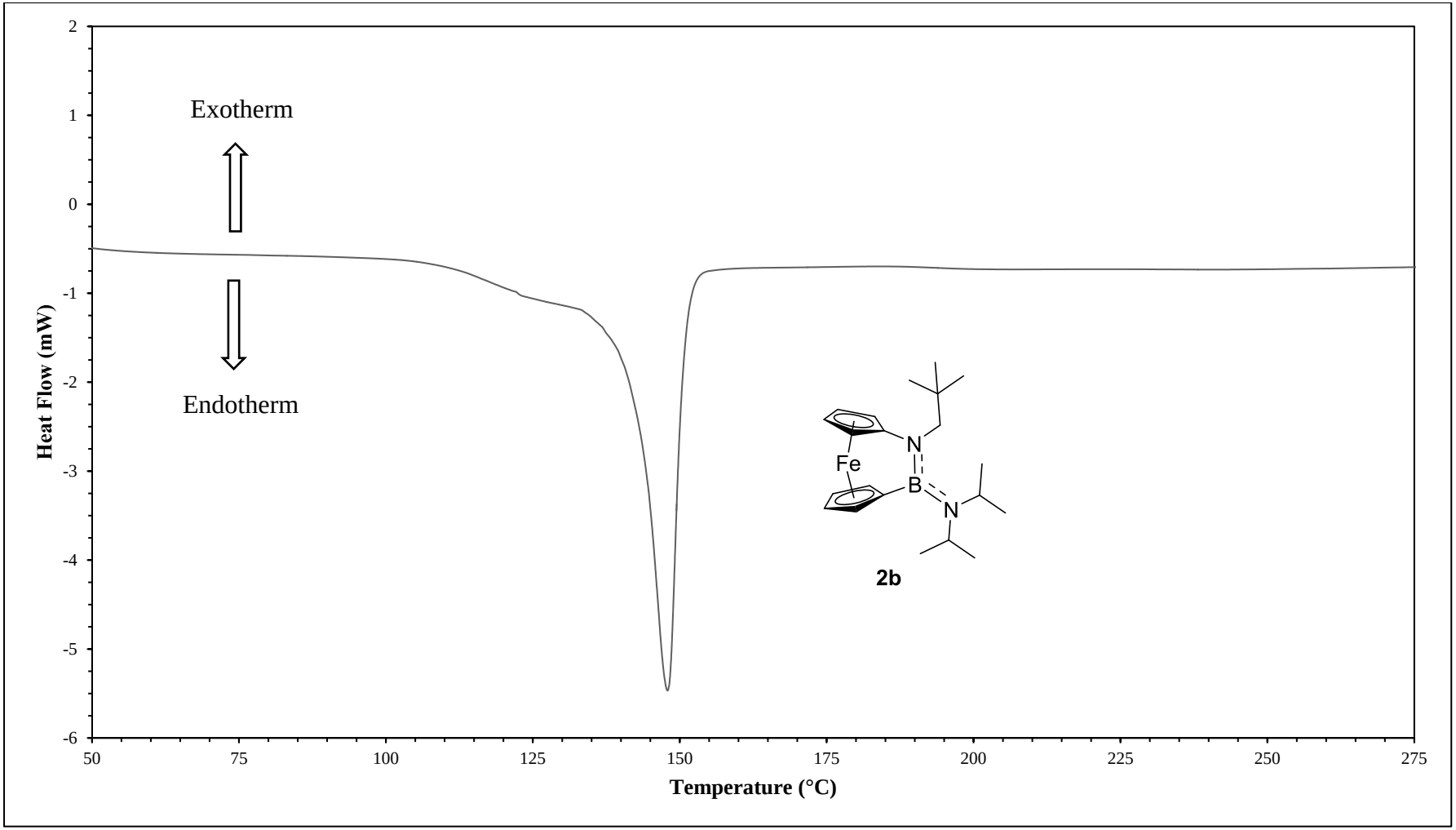

Figure S17. DSC thermogram of **2b**. Heating rate of 10 °C min^{-1}, melting endotherm at T (max) = 148 °C.

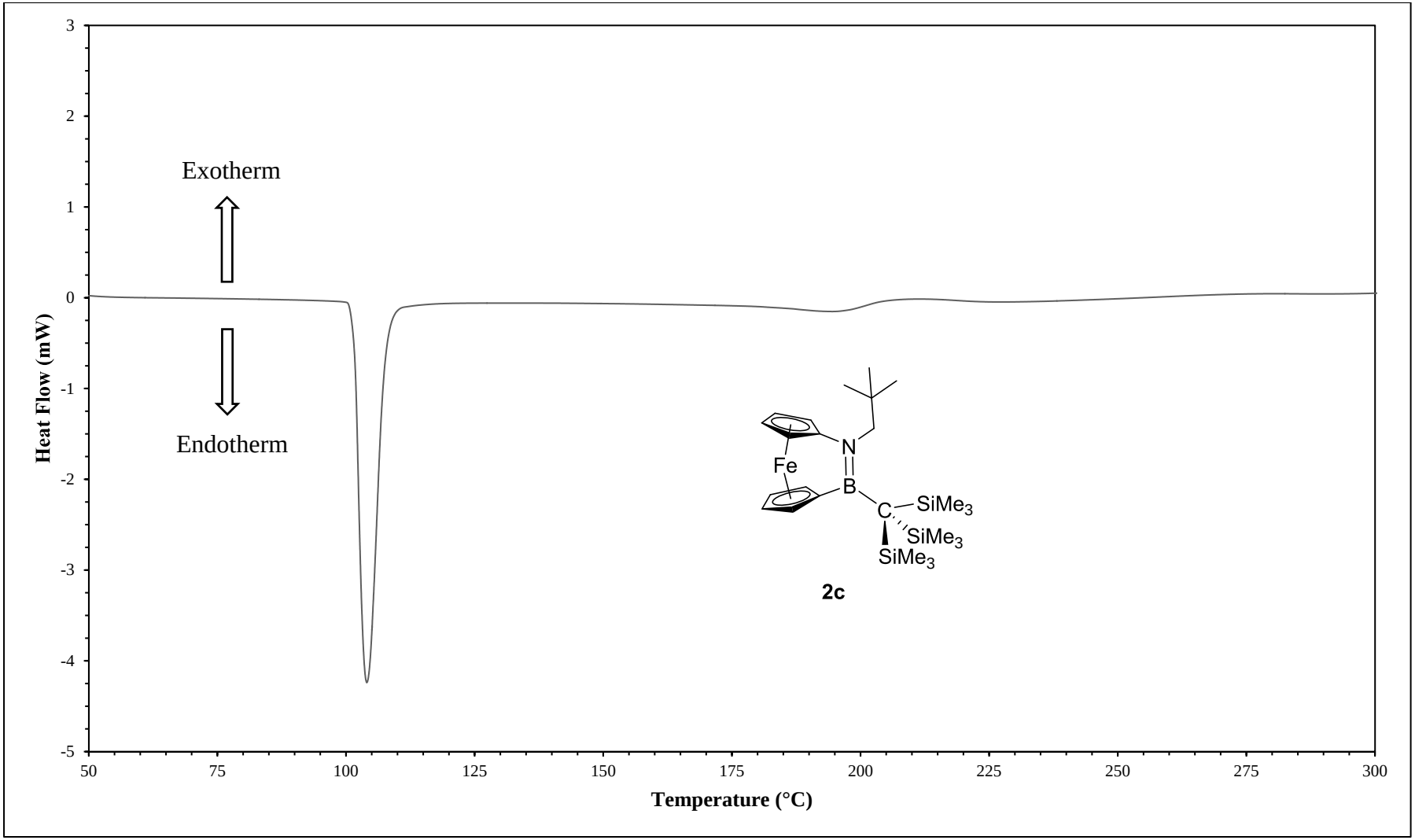

Figure S18. DSC thermogram of **2c**. Heating rate of 10 °C min^{-1}, melting endotherm at T (max) = 104 °C. The change of the position of the baseline around 200 ºC could be due to a 2nd order transition; this was not further investigated. This DSC thermogram and the measured ^{1}H NMR spectrum of the content of the pan revealed that thermal ROP did not occur.